Inorganic Chemistry

Article

pubs.acs.org/IC

Platinum(II) Diimine Complexes with Halide/Pseudohalide Ligands and Dangling Trialkylamine or Ammonium Groups

Sayandev Chatterjee, Jeanette A. Krause, Kumudu Madduma-Liyanage, and William B. Connick*

Department of Chemistry, University of Cincinnati, P.O. Box 210172, Cincinnati, Ohio 45221-0172, United States

Supporting Information

ABSTRACT: A series of platinum(II) complexes with the formulas Pt(diimine)(pip_2NCNH_2)$(L)^{2+}$ [$pip_2NCNH_2^+$ = 2,6-bis(piperidiniummethyl)phenyl cation; L = Cl, Br, I, NCS, OCN, and NO_2; diimine = 1,10-phenanthroline (phen), 5-nitro-1,10-phenanthroline (NO_2phen), and 5,5′-ditrifluoromethyl-2,2′-bipyridine (dtfmbpy)] were prepared by the treatment of Pt(pip_2NCN)Cl with a silver(I) salt followed by the addition of the diimine and halide/pseudohalide under acidic conditions. Crystallographic data as well as ^{1}H NMR spectra establish that the metal center is bonded to a bidentate phenanthroline and a monodentate halide/pseudohalide. The $pip_2NCNH_2^+$ ligand with protonated piperidyl groups is monodentate and bonded to the platinum through the phenyl ring. Structural and spectroscopic data indicate that the halide/pseudohalide group (L^-) and the metal center in Pt(phen)(pip_2NCNH_2)$(L)^{2+}$ behave as Brønsted bases, forming intramolecular NH···L/NH···Pt interactions involving the piperidinium groups. A close examination of the 10 structures reported here reveals linear correlations between N−H···Pt/L angles and H···Pt/L distances. In most cases, the N−H bond is directed toward the Pt−L bond, thereby giving the appearance that the proton bridges the Pt and L groups. In contrast to observations for Pt(tpy)(pip_2NCN)$^+$ (tpy = 2,2′;6′,2″-terpyridine), the electrochemical oxidation of deprotonated adducts, Pt(diimine)(L)(pip_2NCN), is chemically and electrochemically irreversible.

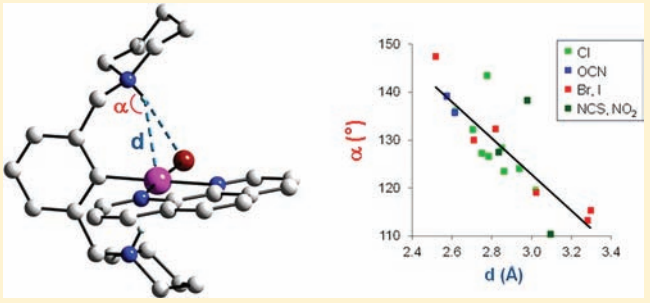

INTRODUCTION

Square-planar d^8-electron and octahedral d^6-electron second- and third-row transition-metal complexes are promising multiredox catalysts because of their tendency to undergo cooperative two-electron changes in the oxidation state coupled to bond-making and bond-breaking steps.[1,2] Fine control of the d^6/d^8 redox potentials would seem a logical strategy for improving catalysts and rationally designing new catalysts. However, surprisingly little is known about the outer-sphere electron-transfer reactions associated with this couple, in large part because these reactions are typically irreversible because of the accompanying drastic changes in the metal coordination sphere. Building on related studies,[3−25] we have prepared Pt(tpy)(pip_2NCN)$^+$ (Scheme 1), which is the first example of a nearly cooperative outer-sphere two-electron platinum reagent.[26,27] In the d^8-electron configuration, the complex possesses two dangling nucleophilic piperidyl groups that can interact with the square-planar metal center and help to stabilize the octahedral coordination geometry preferred by the d^6-electron configuration. The complex undergoes a nearly chemically and electrochemically reversible two-electron oxidation at 0.4 V vs Ag/AgCl (0.1 M $TBAPF_6$ in acetonitrile). The separation between the anodic and cathodic peaks of the oxidation wave (ΔE_p) decreases with the scan rate (150−43 mV; 20.5−0.01 V/s), as expected for an accompanying structural reorganization involving the formation of two Pt^{IV}−piperidyl bonds.

The remarkable near-reversibility of the electrochemistry of Pt(tpy)(pip_2NCN)$^+$ exceeds expectations based on the large geometry change.[26] This observation, as well as spectroscopic and crystallographic data, has led us to suggest that the dangling piperidyl groups interact with the Pt^{II} center prior to or during electron transfer, resulting in a preorganized molecule that undergoes more rapid electron transfer because of its lower Marcus reorganization energy.[28] To better understand the interactions of the metal center with dangling nucleophiles and electrophiles, we have sought to prepare structural and electronic analogues of Pt(tpy)(pip_2NCN)$^+$, such as Pt(phen)$(pipNC)_2$ (Scheme 1).[29] The preparation and handling of such compounds presents challenges because of difficulties in forcing the metal to preferentially bond to one nucleophile over another. We have recently demonstrated that protonation of the dangling nucleophilic groups is an effective strategy for preventing coordination to the metal center.[29] Herein we describe the synthesis and properties of the diprotonated Pt(diimine)(pip_2NCNH_2)$(L)^{2+}$ complexes (Scheme 1), where L^- is a halide or pseudohalide ligand and the diimine ligand is a 1,10-phenanthrolinyl, 5-nitro-1,10-phenanthrolinyl, or 5,5′-ditrifluoromethyl-2,2′-bipyridyl group. The deprotonated adducts, Pt(diimine)(pip_2NCN)(L), can be regarded as close analogues of Pt(tpy)(pip_2NCN)$^+$, in which the terpyridyl ligand

Received: November 15, 2011
Published: April 2, 2012

dx.doi.org/10.1021/ic202462a | Inorg. Chem. 2012, 51, 4572−4587

Scheme 1. Pt(tpy)(pip$_2$NCN)$^+$, Pt(phen)(pipNC)$_2$, and [Pt(diimine)(pip$_2$NCNH$_2$)(L)](PF$_6$)$_2$ (1−8)

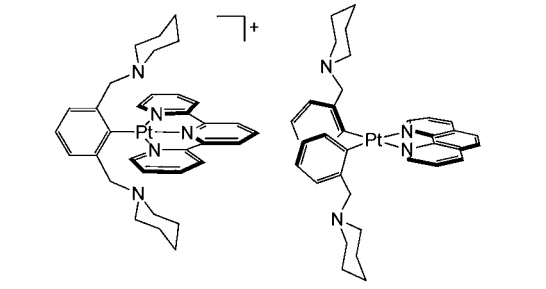

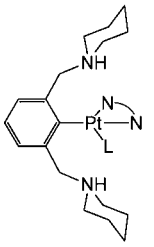

N N	L	Compound
phen	Cl	(1)
phen	Br	(2)
phen	I	(3)
phen	NCS	(4)
phen	NO_2	(5)
phen	OCN	(6)
NO_2phen	Cl	(7)
dtfmbpy	Cl	(8)

[Pt(diimine)(pip$_2$NCNH$_2$)(L)](PF$_6$)$_2$

has been replaced by L$^-$ and a diimine ligand. The results presented here suggest that the metal center in this series of complexes is capable of acting as a Brønsted base and that these interactions have a profound influence on the structural, electronic, and electron-transfer properties.

EXPERIMENTAL SECTION

General Considerations. K_2PtCl_4 was obtained from Pressure Chemical Company (Pittsburgh, PA). 2,2′-Azobis(isobutyronitrile) (AIBN), 2-bromo-*m*-xylene, and 1,5-cyclooctadiene (COD) were obtained from Aldrich Chemical Co. (Milwaukee, WI). All other reagents were purchased from Acros. Tetrahydrofuran (THF) was distilled from sodium metal and benzophenone, and ethanol was distilled from zinc metal and potassium hydroxide. All other chemicals were used as received. Pt(COD)Cl$_2$,[30] Pt(DMSO)$_2$Cl$_2$,[31] 2,6-*bis*(bromomethyl)bromobenzene,[32] 2,6-[CH$_2$(C$_5$H$_{10}$N)]$_2$C$_6$H$_3$Br (pip$_2$NCNBr),[33] 2-[CH$_2$(C$_5$H$_{10}$N)]C$_6$H$_4$ (pipNCH),[29] 5,5′-di-(trifluoromethyl)-2,2′-bipyridine (dtfmbpy),[34] and Pt(pip$_2$NCN)Cl[35] and Pt(pipNC)(DMSO)Cl[36] [pip$_2$NCN$^-$ = 2,6-*bis*(piperidylmethyl)-phenyl anion; pipNC$^-$ = 2-(piperidylmethyl)phenyl anion] were prepared according to literature procedures. Syntheses involving amines were carried out in an inert argon atmosphere using standard Schlenk techniques. Argon was pre-dried using activated sieves, and trace impurities of oxygen were removed with activated R3-11 catalyst from Schweizerhall.

^{1}H NMR spectra were recorded at room temperature using a Bruker AC 400 MHz instrument. Deuterated solvents, $CDCl_3$ [0.03% (v/v) tetramethylsilane (TMS)], CD_2Cl_2 [0.05% (v/v) TMS], and CD_3CN, were purchased from Cambridge Isotope Laboratories. Spectra are reported in parts per million (ppm) relative to TMS (δ = 0 ppm) for $CDCl_3$ and CD_2Cl_2 or relative to the protic solvent impurity in the case of CD_3CN (δ = 1.94 ppm for CD_2HN). Elemental analysis was performed by Atlantic Microlab, Inc. (Norcross, GA). UV−visible absorption spectra were recorded using a HP8453 UV−visible diode-array spectrometer. Emission spectra were recorded using a SPEX Fluorolog-3 fluorimeter equipped with a double-emission monochromator (385 nm cutoff filter) and a single excitation monochromator. Glassy solutions (77 K) were prepared by inserting a quartz electron paramagnetic resonance tube containing a *N*-butyronitrile solution of the respective complex into a quartz-tipped finger dewar. Emission spectra were corrected for instrumental response. Mass spectra were obtained by electrospray ionization (ESI) of acetonitrile solutions using a Micromass Q-TOF-2 instrument.

Cyclic voltammetry measurements were carried out using a standard three-electrode cell and a 100 B/W electrochemical workstation from Bioanalytical Systems. Scans were recorded on CH_2Cl_2 solutions containing 0.1 M $TBAPF_6$. All scans were recorded using a platinum wire auxiliary electrode and a 0.79 mm^2 gold working electrode. Scans recorded using platinum and glassy carbon working electrodes were significantly broadened, suggesting poorer electrochemical reversibility. Between measurements, the working electrode was polished with 0.05 μm alumina, rinsed with distilled water, and wiped dry using a Kimwipe. Reported potentials are referenced vs Ag/AgCl (3.0 M NaCl). Peak currents (i_p) were estimated with respect to the extrapolated baseline current, as described by Kissinger and Heineman.[37] Under these conditions, the ferrocene/ferrocenium (Fc/Fc$^+$) couple occurs at 0.51 V (ΔE_p, 68 mV; 0.10 V/s).

[Pt(phen)(pip$_2$NCNH$_2$)Cl](PF$_6$)$_2$ (1). $AgPF_6$ (25 mg, ∼0.1 mmol) was added to a solution of Pt(pip$_2$NCN)Cl (50 mg, 0.1 mmol) in CH_3CN, and the mixture was stirred in the dark for 1 h. The resulting precipitate was removed by filtration through Celite. Trifluoroacetic acid (14.7 μL, 0.2 mmol) was added to the pale-yellow filtrate, followed by the addition of 1,10-phenanthroline (phen; 18 mg, 0.1 mmol) and KCl (8 mg, 0.1 mmol). The mixture was refluxed for 2 h and then filtered. Excess NH_4PF_6 was added to the filtrate, and the mixture was filtered again to remove residual NH_4PF_6. The filtrate was rotary evaporated to one-third of the initial volume, excess diethyl ether was added, and the solution was cooled in a refrigerator. The resulting pale-yellow precipitate was collected and washed with water to give a pale-yellow powder. Yield: 0.066 g, 68%. ^{1}H NMR (CD_3CN, δ): 1.42 (2H, m, aliphatic pip$_2$NCNH$_2$), 1.62 (2H, m, aliphatic pip$_2$NCNH$_2$), 1.77 (4H, m, aliphatic pip$_2$NCNH$_2$), 1.87 (4H, m, aliphatic pip$_2$NCNH$_2$), 2.84 (2H, dd, aliphatic pip$_2$NCNH$_2$ α-H, J_{H-H} = 14.8 and 12.0 Hz), 3.03 (2H, dd, aliphatic pip$_2$NCNH$_2$ α-H, J_{H-H} = 15.2 and 11.6 Hz), 3.29 (2H, dd, aliphatic pip$_2$NCNH$_2$ α-H, J_{H-H} = 11.6 and 2 Hz), 3.64 (2H, dd, aliphatic pip$_2$NCNH$_2$ α-H, J_{H-H} = 10.8 and 4 Hz), 4.17 (2H, dd, benzylic CH$_2$, J_{H-H} = 12.8 and 2.0 Hz), 4.95 (2H, dd, benzylic CH$_2$, J_{H-H} = 12.8 and 2.0 Hz), 7.29 (1H, t, aromatic pip$_2$NCNH$_2$, J_{H-H} = 8.0 Hz), 7.41 (2H, d, aromatic pip$_2$NCNH$_2$, J_{H-H} = 8.0 Hz), 7.66 (1H, d, phen, J_{H-H} = 6.8 Hz), 7.67 (1H, d, phen, J_{H-H} = 6.8 Hz), 7.94 (1H, dd with Pt satellites, phen, J_{H-Pt} = 61 Hz, J_{H-H} = 6.8 and 1.2 Hz), 8.20 (1H, t, phen, J_{H-H} = 6.8 Hz), 8.21 (2H, s, N−H), 8.22 (1H, t, phen, J_{H-H} = 6.8 Hz), 8.82 (1H, dd, phen, J_{H-H} = 8.4 and 0.8 Hz), 8.92 (1H, dd, phen, J_{H-H} = 8.4 and 0.8 Hz), 9.48 (1H, dd, phen, J_{H-H} = 6.8 and 0.8 Hz). ^{1}H NMR (CD_2Cl_2, δ): 0.72−1.52 (m, aliphatic pip$_2$NCNH$_2$ overlapping with solvent resonances), 1.52−1.98 (8H, m, aliphatic pip$_2$NCNH$_2$ β-H), 2.81 (2H, dd, aliphatic pip$_2$NCNH$_2$ α-H, J_{H-H} = 20.0 and 7.6 Hz), 3.05 (2H, dd, aliphatic pip$_2$NCNH$_2$ α-H, J_{H-H} = 24.0 and 8.0 Hz), 3.33 (2H, dd, aliphatic pip$_2$NCNH$_2$ α-H, J_{H-H} = 24.0 and 8.0 Hz), 3.69 (2H, dd, aliphatic pip$_2$NCNH$_2$ α-H, J_{H-H} = 11.2 and 3.6 Hz), 4.10 (2H, dd, benzylic CH$_2$, J_{H-H} = 14.0 and 9.6 Hz), 5.15 (2H, dd, benzylic CH$_2$, J_{H-H} = 13.2 and 1.2 Hz), 7.28 (1H, t, aromatic pip$_2$NCNH$_2$, J_{H-H} = 8.0 Hz), 7.37 (2H, d, aromatic pip$_2$NCNH$_2$, J_{H-H} = 8.0 Hz), 7.39 (2H, s, N−H), 7.58 (1H, dd, phen, J_{H-H} = 8.0 and 5.6 Hz), 7.79 (1H, dd, phen, J_{H-H} = 5.2 and 0.8 Hz), 8.07 (3H, m, phen), 8.65 (1H, dd, phen, J_{H-H} = 8.0 and 0.8 Hz), 8.74 (1H, dd, phen, J_{H-H} = 4.2 and 1.5 Hz), 9.37 (1H, dd, phen, J_{H-H} = 4.0 and 1.2 Hz). MS-ESI (m/z). Obsd (calcd): 323.63 (323.63), [Pt(phen)(pip$_2$NCNH)]$^{2+}$; 341.62 (341.62), [Pt(phen)(pip$_2$NCNH$_2$)Cl]$^{2+}$; 828.20 (828.20), [Pt(phen)(pip$_2$NCNH$_2$)Cl](PF$_6$)$^+$.

[Pt(phen)(pip$_2$NCNH$_2$)Br](PF$_6$)$_2$ (2). The product was isolated as a bright-yellow solid following the same procedure as that for **1** and substituting KBr (12 mg, 0.1 mmol) for KCl. Yield: 0.066 g, 64%. ^{1}H NMR (CD_3CN, δ): 1.47−1.77 (m, aliphatic pip$_2$NCNH$_2$ overlapping with solvent resonances), 2.87 (2H, dd, aliphatic pip$_2$NCNH$_2$ α-H, J_{H-H} = 24.8 and 12.8 Hz), 3.04 (2H, dd, aliphatic pip$_2$NCNH$_2$ α-H, J_{H-H} = 25.6 and 10.4 Hz), 3.32 (2H, dd, aliphatic pip$_2$NCNH$_2$ α-H, J_{H-H} = 12.4 and 4.0 Hz), 3.62 (2H, dd, aliphatic pip$_2$NCNH$_2$ α-H,

dx.doi.org/10.1021/ic202462a | Inorg. Chem. 2012, 51, 4572−4587

J_{H-H} = 12.4 and 4.0 Hz), 4.18 (2H, dd, benzylic CH_2, J_{H-H} = 13.6 and 6.0 Hz), 4.91 (2H, dd, benzylic CH_2, J_{H-H} = 12.4 and 1.6 Hz), 7.27 (1H, t, aromatic pip_2NCNH_2, J_{H-H} = 5.2 Hz), 7.41 (2H, d, aromatic pip_2NCNH_2, J_{H-H} = 5.2 Hz), 7.47 (2H, s, N−H), 7.69 (1H, dd, phen, J_{H-H} = 8.0 and 6.48 Hz), 7.88 (1H, dd with Pt satellites, phen, J_{H-Pt} ∼ 60 Hz, J_{H-H} = 5.6 and 1.2 Hz), 8.20 (2H, t, phen, J_{H-H} = 8.4 Hz), 8.23 (1H, dd, phen, J_{H-H} = 8.0 and 1.2 Hz), 8.83 (1H, dd, phen, J_{H-H} = 8.0 and 1.2 Hz), 8.91 (1H, dd, phen, J_{H-H} = 8.4 and 1.2 Hz), 9.68 (1H, dd, phen, J_{H-H} = 4.8 and 1.6 Hz). ^{1}H NMR (CD_2Cl_2, δ): 0.59−1.98 (m overlapping with solvent resonances, aliphatic pip_2NCNH_2), 2.85 (2H, dd, aliphatic pip_2NCNH_2 α-H, J_{H-H} = 25.2 and 12.0 Hz), 3.09 (2H, dd, aliphatic pip_2NCNH_2 α-H, J_{H-H} = 26.0 and 10.8 Hz), 3.37 (2H, dd, aliphatic pip_2NCNH_2 α-H, J_{H-H} = 12.0 and 4.4 Hz), 3.65 (2H, dd, aliphatic pip_2NCNH_2 α-H, J_{H-H} = 12.2 and 2.0 Hz), 4.11 (2H, dd, benzylic CH_2, J_{H-H} = 12.8 and 10.8 Hz), 5.03 (2H, dd, benzylic CH_2, J_{H-H} = 12.4 and 0.8 Hz), 7.24 (1H, t, aromatic pip_2NCNH_2, J_{H-H} = 8.0 Hz), 7.37 (2H, d, aromatic pip_2NCNH_2, J_{H-H} = 8.0 Hz), 7.42 (2H, s, N−H), 7.60 (1H, dd, phen, J_{H-H} = 9.2 and 5.6 Hz), 7.72 (1H, dd, phen, J_{H-H} = 4.8 and 2.4 Hz), 8.08 (2H, phen, m), 8.67 (1H, dd, phen, J_{H-H} = 8.0 and 1.2 Hz), 8.73 (1H, dd, phen, J_{H-H} = 8.0 and 2.0 Hz), 9.57 (1H, d, phen, J_{H-H} = 6.0 Hz). MS-ESI (m/z). Obsd (calcd): 323.63 (323.63), $[Pt(phen)(pip_2NCNH)]^{2+}$; 364.59 (364.59), $[Pt(phen)(pip_2NCNH_2)Br]^{2+}$; 874.15 (874.15), $[Pt(phen)(pip_2NCNH_2)Br](PF_6)^+$.

$[Pt(phen)(pip_2NCNH_2)I](PF_6)_2$ (3). The product was isolated as a bright-yellow solid following the same procedure as that for **1**, substituting KI (17 mg, ∼0.1 mmol) for KCl, and stirring the solution at room temperature overnight instead of heating. Yield: 0.070 g, 66%. ^{1}H NMR (CD_3CN, δ): 1.42 (2H, m), 1.60−1.86 (m, aliphatic pip_2NCNH_2 overlapping with solvent resonances), 2.83 (2H, dd, aliphatic pip_2NCNH_2 α-H, J_{H-H} = 24.4 and 11.2 Hz), 3.00 (2H, dd, aliphatic pip_2NCNH_2 α-H, J_{H-H} = 22.0 and 11.2 Hz), 3.33 (2H, dd, aliphatic pip_2NCNH_2 α-H, J_{H-H} = 12.4 and 2.4 Hz), 3.52 (2H, dd, aliphatic pip_2NCNH_2 α-H, J_{H-H} = 12.0 and 2.8 Hz), 4.35 (2H, dd, benzylic CH_2, J_{H-H} = 13.2 and 8.0 Hz), 4.75 (2H, dd, benzylic CH_2, J_{H-H} = 13.2 and 1.2 Hz), 7.25 (1H, t, aromatic pip_2NCNH_2, J_{H-H} = 7.6 Hz), 7.39 (2H, d, aromatic pip_2NCNH_2, J_{H-H} = 7.6 Hz), 7.53 (2H, s, N−H), 7.75 (1H, dd, phen, J_{H-H} = 8.8 and 5.6 Hz), 7.87 (1H, dd, phen, J_{H-H} = 6.8 and 1.2 Hz), 8.18 (1H, dd with Pt satellites, phen, J_{H-Pt} = 62 Hz, J_{H-H} = 8.8 and 4.4 Hz), 8.23 (2H, t, phen, J_{H-H} = 6.8 Hz), 8.89 (2H, dd, phen, J_{H-H} = 4.4 and 2.0 Hz), 10.03 (1H, dd, phen, J_{H-H} = 5.2 and 1.6 Hz). MS-ESI (m/z). Obsd (calcd): 387.57 (387.59), $[Pt(phen)(pip_2NCNH_2)I]^{2+}$; 774.17 (774.16), $[Pt(phen)(pip_2NCNH)I]^+$; 920.14 (920.14), $[Pt(phen)(pip_2NCNH_2)I](PF_6)^+$.

$[Pt(phen)(pip_2NCNH_2)(NCS)](PF_6)_2$ (4). The product was isolated as a pale-yellow solid following the same procedure as that for **3** and substituting KSCN (10 mg, ∼0.1 mmol) for KI. Yield: 0.070 g, 70%. ^{1}H NMR (CD_3CN, δ): 0.88 (2H, m, aliphatic pip_2NCNH_2), 1.42−2.02 (m, aliphatic pip_2NCNH_2 overlapping with solvent resonances), 2.86 (2H, dd, aliphatic pip_2NCNH_2 α-H, J_{H-H} = 14.4 and 12.4 Hz), 3.05 (2H, dd, aliphatic pip_2NCNH_2 α-H, J_{H-H} = 14.4 and 12.4 Hz), 3.32 (2H, dd, aliphatic pip_2NCNH_2 α-H, J_{H-H} = 12.4 and 2.4 Hz), 3.64 (2H, dd, aliphatic pip_2NCNH_2 α-H, J_{H-H} = 12.4 and 2.4 Hz), 4.14 (2H, dd, benzylic CH_2, J_{H-H} = 12.8 and 2.0 Hz), 4.92 (2H, dd, benzylic CH_2, J_{H-H} = 12.8 and 2 Hz), 7.29 (2H, d, aromatic pip_2NCNH_2, J_{H-H} = 7.6 Hz), 7.38 (1H, t, aromatic pip_2NCNH_2, J_{H-H} = 7.2 Hz), 7.59 (1H, d, phen, J_{H-H} = 7.6 Hz), 7.66 (1H, d, phen, J_{H-H} = 5.6 Hz), 7.92 (1H, dd, phen, J_{H-H} = 4.8 and 2.0 Hz), 8.22 (1H, t, phen, J_{H-H} = 7.6 Hz), 8.24 (1H, t, phen, J_{H-H} = 8.0 Hz), 8.21 (2H, bs, N−H), 8.80 (1H, dd, phen, J_{H-H} = 4.8 and 2.0 Hz), 8.92 (1H, dd, phen, J_{H-H} = 4.4 and 2.0 Hz), 9.49 (1H, dd, phen, J_{H-H} = 8.0 and 1.2 Hz). MS-ESI (m/z). Obsd (calcd): 353.12(353.12), $[Pt(phen)(pip_2NCNH_2)(NCS)]^{2+}$; 705.24 (705.23), $[Pt(phen)(pip_2NCNH)(NCS)]^+$.

$[Pt(phen)(pip_2NCNH_2)(NO_2)](PF_6)_2$ (5). The product was isolated as a pale-yellow solid following the same procedure as that for **1** and substituting KNO_2 (9 mg, ∼0.1 mmol) for KCl. Yield: 0.070 g, 71%. ^{1}H NMR (CD_3CN, δ): 1.47 (2H, m, aliphatic pip_2NCNH_2), 1.66 (2H, m, aliphatic pip_2NCNH_2), 1.78−1.91 (8H, m, aliphatic pip_2NCNH_2), 2.88 (2H, dd, aliphatic pip_2NCNH_2 α-H, J_{H-H} = 14.4 and 12.4 Hz), 3.04 (2H, dd, aliphatic pip_2NCNH_2 α-H, J_{H-H} = 14.0 and 10.0 Hz), 3.31 (2H, d, aliphatic pip_2NCNH_2 α-H, J_{H-H} = 12.8 Hz), 3.71 (2H, d, aliphatic pip_2NCNH_2 α-H, J_{H-H} = 12.0 Hz), 4.26 (2H, dd, benzylic CH_2, J_{H-H} = 12.8 and 0.4 Hz), 4.98 (2H, dd, benzylic CH_2, J_{H-H} = 13.2 and 0.4 Hz), 7.35 (1H, dd, aromatic pip_2NCNH_2, J_{H-H} = 8.4 and 6.8 Hz), 7.45 (2H, d, aromatic pip_2NCNH_2, J_{H-H} = 7.6 Hz), 7.70 (1H, dd, phen, J_{H-H} = 8.0 and 5.6 Hz), 7.84 (1H, dd with Pt satellites, phen, J_{H-Pt} = 40 Hz, J_{H-H} = 5.6 and 1.2 Hz), 8.17 (1H, dd, phen, J_{H-H} = 8.4 and 5.2 Hz), 8.18 (2H, bs, N−H), 8.20 (1H, d, phen, J_{H-H} = 9.2 Hz), 8.27 (1H, d, phen, J_{H-H} = 9.2 Hz), 8.80 (1H, dd, phen, J_{H-H} = 5.6 and 1.2 Hz), 8.81 (1H, d, phen, J_{H-H} = 2.0 and 1.6 Hz), 8.97 (1H, dd, phen, J_{H-H} = 8.0 and 1.2 Hz). MS-ESI (m/z). Obsd (calcd): 347.12 (347.13), $[Pt(phen)(pip_2NCNH_2)(NO_2)]^{2+}$; 693.25 (693.25), $[Pt(phen)(pip_2NCNH)(NO_2)]^+$; 839.22 (839.22), $[Pt(phen)(pip_2NCNH_2)(NO_2)](PF_6)^+$.

$[Pt(NO_2phen)(pip_2NCNH_2)Cl](PF_6)_2$ (7). The product was isolated as a lemon-yellow solid following the same procedure as that for **1** and substituting 5-nitro-1,10-phenanthroline (NO_2phen; 23 mg, 0.1 mmol) for phen. Yield: 0.065 g, 64%. ^{1}H NMR (CD_3CN, δ): 1.47 (2H, m, aliphatic pip_2NCNH_2), 1.61 (2H, m, aliphatic pip_2NCNH_2), 1.71−1.94 (m, aliphatic pip_2NCNH_2 overlapping with solvent resonances), 2.87 (2H, dd, aliphatic pip_2NCNH_2 α-H, J_{H-H} = 10.0 and 4.0 Hz), 3.06 (2H, dd, aliphatic pip_2NCNH_2 α-H, J_{H-H} = 9.2 and 5.6 Hz), 3.29 (2H, dd, aliphatic pip_2NCNH_2 α-H, J_{H-H} = 9.2 and 5.6 Hz), 3.66 (2H, dd, aliphatic pip_2NCNH_2 α-H, J_{H-H} = 12.4 and 2.4 Hz), 4.16 (2H, dd, benzylic CH_2, J_{H-H} = 17.6 and 4.8 Hz), 4.94 (2H, dd, benzylic CH_2, J_{H-H} = 11.6 and 4.8 Hz), 7.31 (1H, t, aromatic pip_2NCNH_2, J_{H-H} = 7.2 Hz), 7.41 (2H, d, aromatic pip_2NCNH_2, J_{H-H} = 6.8 Hz), 7.47 (2H, bs, N−H), 7.78 (1H, dd, NO_2phen, J_{H-H} = 13.6 and 4.8 Hz), 8.08 (1H, dd with Pt satellites, NO_2phen, J_{H-Pt} = 56 Hz, J_{H-H} = 9.6 and 1.2 Hz), 8.38 (1H, d, NO_2phen, J_{H-H} = 6.0 Hz), 9.01 (1H, d, NO_2phen, J_{H-H} = 8.0 Hz), 9.15 (1H, s, NO_2phen), 9.46 (1H, d, NO_2phen, J_{H-H} = 8.0 Hz), 9.63 (1H, dd, J_{H-H} = 9.6 and 1.2 Hz). MS-ESI (m/z). Obsd (calcd): 363.61 (363.61), $[Pt(NO_2phen)(pip_2NCNH_2)Cl]^{2+}$; 874.18 (874.18), $[Pt(NO_2phen)(pip_2NCNH_2)Cl](PF_6)^+$.

$[Pt(dtfmbpy)(pip_2NCNH_2)Cl](PF_6)_2$ (8). The product was isolated as a bright-yellow solid following the same procedure as that for **1** and substituting dtfmbpy (30 mg, ∼0.1 mmol) for phen. Yield: 0.060 g, 55%. ^{1}H NMR spectra showed two sets of closely overlapping resonances in a 3:2 intensity ratio. ^{1}H NMR (CD_3CN, δ): 1.54 (2.4H, m, aliphatic pip_2NCNH_2), 1.62 (1.6H, m, aliphatic pip_2NCNH_2), 1.77−2.10 (m, aliphatic pip_2NCNH_2 overlapping with solvent resonances), 2.75 (0.8H, dd, aliphatic pip_2NCNH_2, J_{H-H} = 12.4 and 2.4 Hz), 2.88 (1.2H, dd, aliphatic pip_2NCNH_2, J_{H-H} = 12.4 and 2.4 Hz), 3.11−3.24 (4H, m, aliphatic pip_2NCNH_2), 3.72 (2H, dd, aliphatic pip_2NCNH_2), 3.87 (0.8H, dd, benzylic CH_2, J_{H-H} = 13.6 and 4.8 Hz), 4.20 (1.2H, dd, benzylic CH_2, J_{H-H} = 13.6 and 4.8 Hz), 4.60 (0.8H, dd, benzylic CH_2, J_{H-H} = 11.6 and 4.8 Hz), 5.00 (1.2H, dd, benzylic CH_2, J_{H-H} = 11.6 and 4.8 Hz), 6.91 (0.6H, dd, J_{H-H} = 9.6 and 4.8 Hz), 6.97 (0.4H, dd, J_{H-H} = 9.6 and 4.8 Hz), 7.35−7.44 (5H, m, aromatic protons overlapping with N−H resonances), 7.57 (1.2H, m), 7.75 (0.8H, m), 8.64−8.74 (2H, m), 9.52 (0.6H, d, J_{H-H} = 8.0 Hz), 9.55 (0.4H, d, J_{H-H} = 8.0 Hz). MS-ESI (m/z). Obsd (calcd): 397.11 (397.10), $[Pt(dtfmbpy)(pip_2NCNH_2)Cl]^{2+}$; 941.18 (941.18), $[Pt(dtfmbpy)(pip_2NCNH_2)Cl](PF_6)^+$.

Pt(pipNC)(DMSO)Cl. A solution of sodium acetate (0.32 g, 2.4 mmol), pipNCH (0.415 g, 2.4 mmol), and $Pt(DMSO)_2Cl_2$ (1.0 g, 2.4 mmol) in 75 mL of methanol was stirred for 4 days at room temperature. After rotary evaporation, the residue was treated with water (25 mL) and extracted with CH_2Cl_2 (3 × 50 mL). The combined CH_2Cl_2 layers were dried over $MgSO_4$, filtered, and rotary evaporated to dryness. The residue was purified by column chromatography (silica: 10 in. length, 1.25 in. diameter, 19:1 $CHCl_3$/acetone). The product was further purified by vapor diffusion of diethyl ether into a methylene chloride solution to give an off-white solid. Yield: 0.44 g, 39%. Anal. Calcd for $(C_{12}H_{16}N)(C_2H_6SO)PtCl$: C, 34.82; H, 4.59; N, 2.90. Found: C, 34.57; H, 4.52; N, 2.92. ^{1}H NMR ($CDCl_3$, δ): 1.42−1.92 (6H, m, CH_2), 3.13 (2H, m, CH_2), 3.55 (6H, s with Pt satellites, J_{H-Pt} = 25 Hz, CH_3), 3.92 (2H, m, CH_2), 4.28 (2H, s

dx.doi.org/10.1021/ic202462a | Inorg. Chem. 2012, 51, 4572−4587

Scheme 2. Synthesis of Pt(diimine)(pip_2NCNH_2)(L)$^{2+a}$

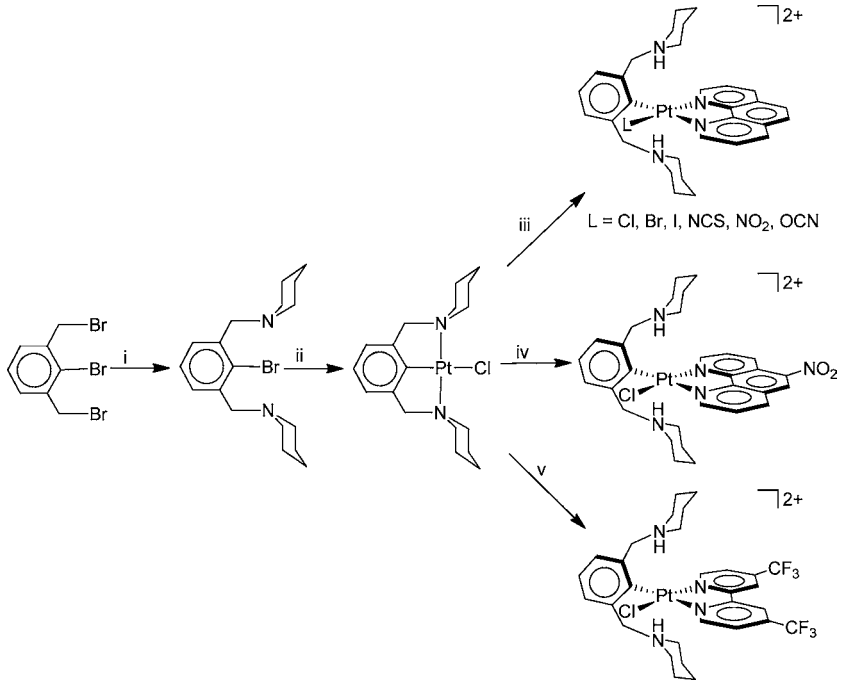

[a](i) Piperidine/benzene; (ii) ^{n}BuLi, Pt(COD)Cl_2/THF, −70 °C; (iii−v) TFA, diimine, KL/CH_3CN.

with Pt satellites, J_{H-Pt} = 45 Hz, CH_2), 6.99−7.13 (3H, m, CH), 7.92 (2H, d with Pt satellites, J_{H-Pt} = 47 Hz, CH).

[Pt(phen)(pipNHC)Cl](BF$_4$) (9). The product was isolated as a pale-yellow solid following the same procedure as that for [(pip_2NCNH_2)Pt(phen)Cl](PF_6)$_2$ and substituting Pt(pipNC)(DMSO)Cl (49 mg, ∼0.1 mmol) for Pt(pip_2NCN)Cl and $AgBF_4$ (19 mg, ∼0.1 mmol) for $AgPF_6$. Yield: 0.035 g, 52%. ^{1}H NMR (CD_3CN, δ): 1.43 (2H, m), 1.61 (2H, m), 1.77 (4H, m, aliphatic pipNHC), 1.87 (4H, m, aliphatic pipNHC), 2.85 (1H, dd, aliphatic pipNHC α-H, J_{H-H} = 14.4 and 12.0 Hz), 3.00 (1H, dd, aliphatic pipNHC α-H, J_{H-H} = 14.8 and 12.0 Hz), 3.30 (1H, dd, aliphatic pipNHC α-H, J_{H-H} = 11.6 and 2.0 Hz), 3.61 (1H, dd, aliphatic pipNHC α-H, J_{H-H} = 10.0 and 2.0 Hz), 4.04 (1H, dd, benzylic CH_2, J_{H-H} = 12.8 and 2.0 Hz), 4.70 (1H, dd, benzylic CH_2, J_{H-H} = 12.0 and 2.0 Hz), 7.13 (1H, t, aromatic pipNHC, J_{H-H} = 8.0 Hz), 7.23 (2H, d, aromatic pipNHC, J_{H-H} = 8.0 Hz), 7.49 (1H, d, phen, J_{H-H} = 6.8 Hz), 7.68 (1H, d, phen, J_{H-H} = 6.8 Hz), 8.05 (1H, dd with Pt satellites, aromatic pipNHC, J_{H-Pt} = 56 Hz, J_{H-H} = 6.8 and 1.2 Hz), 8.24 (2H, t, phen, J_{H-H} = 6.0 Hz), 8.32 (1H, t, phen, J_{H-H} = 6.8 Hz), 8.35 (1H, s, N−H), 8.78 (1H, dd, phen, J_{H-H} = 8.4 and 0.8 Hz), 8.85 (1H, dd, phen, J_{H-H} = 8.4 and 0.8 Hz), 9.54 (1H, dd, phen, J_{H-H} = 6.8 and 0.8 Hz). MS-ESI (m/z). Obsd (calcd): 585.15 (585.14), [(pipNHC)Pt(phen)Cl]$^+$; 637.17 (637.17), [(pipNHC)Pt(phen)](BF$_4$)$^+$.

Pt(phen)(pip_2NCN)Cl. The complex was generated in situ by adding 2 equiv of KOH (1.0 mM in CD_3OD) to a 0.5 mM solution of **1** in CD_2Cl_2 or by adding 2 equiv of TBAOH (1.0 mM) to a 0.5 mM solution of **1** in CD_3CN. Excess base resulted in decomposition. ^{1}H NMR (CD_2Cl_2, δ): 0.75−3.70 (m, aliphatic pip_2NCN overlapping with solvent resonances), 4.11 (2H, d, benzylic CH_2), 4.14 (2H, d, benzylic CH_2), 6.69 (2H, d, aromatic pip_2NCN, J_{H-H} = 6.8 Hz), 6.81 (1H, t, aromatic pip_2NCN, J_{H-H} = 7.6 Hz), 7.61 (2H, dd, phen, J_{H-H} = 8.0 and 4.4 Hz), 7.78 (2H, s, phen), 8.25 (2H, d, phen, J_{H-H} = 8.0 Hz), 9.04 (2H, d, phen, J_{H-H} = 3.6 Hz). ^{1}H NMR (CD_3CN, δ): 0.8−4.0 (m, aliphatic pip_2NCN overlapping solvent resonances and resonances from TBA^+ cation of the base), 4.32 (bs, benzylic CH_2), 7.12 (4H, m, aromatic pip_2NCN overlapping with phen resonance), 7.65 (1H, m, phen), 8.17 (3H, m, phen), 8.77 (1H, t, phen, J_{H-H} = 8.8 Hz), 8.86 (1H, t, phen, J_{H-H} = 8.4 Hz), 9.64 (1H, m, phen).

X-ray Crystallography. Single crystals of the hexafluorophosphate salts of Pt(phen)(pip_2NCNH_2)(L)$^{2+}$ [L = Cl (**1**), Br (**2**), I (**3**), NCS (**4**), NO_2 (**5**), and Pt(dtfmbpy)(pip_2NCNH_2)Cl^{2+} (**8**)], as well as the BF_4^- salt of Pt(phen)(pipNHC)Cl^+ (**9**), were obtained from CH_3CN/Et_2O. In the case of Pt(phen)(pip_2NCNH_2)Cl^{2+}, a crystal form containing CH_3CN and H_2O solvate also was obtained as pale-yellow blocks from CH_3CN/CH_2Cl_2/Et_2O (**1**·0.25CH_3CN·0.5H_2O). In the case of crystals containing [Pt(phen)(pip_2NCNH_2)(OCN)](PF)$_2$ (**6**), a yellow solid was isolated by following the same procedure as that for **1** and substituting KNCO (8 mg, ∼0.1 mmol) for KCl; single crystals were obtained by vapor diffusion of Et_2O into a CH_3CN solution of the product. Single crystals of **7**·0.25CH_3OH were obtained from CH_3CN/Et_2O/CH_3OH. For X-ray examination and data collection, suitable crystals of appropriate dimensions were mounted in a loop with paratone-N and transferred immediately to the goniostat bathed in a cold stream.

Low-temperature intensity data were collected using synchrotron radiation (λ = 0.775 Å) with either a Bruker Platinum 200 or APEX2 CCD detector at Beamline 11.3.1 at the Advanced Light Source (Lawrence Berkeley National Laboratory) or using Cu Kα radiation (λ = 1.54178 Å) with a Bruker SMART6000 CCD diffractometer. Data frames were collected using the *APEX2* or *SMART* programs, respectively, and processed using *SAINT*. The data were corrected for absorption and beam corrections based on the multiscan technique as implemented in SADABS. The structures were solved by a combination of either direct methods or the Patterson method using *SHELXTL* or *SIR2004*, expanded using the difference Fourier technique, and refined by full-matrix least squares on F^2. Non-H atoms were refined with anisotropic displacement parameters with the exception of the disordered F atoms in **2** and the solvate in **7**·0.25CH_3OH. The NH piperidinium and water solvate H atoms were located directly from the difference map and held fixed at that location in subsequent refinement cycles; the one exception is **1**·0.25CH_3CN·0.5H_2O, for which the position of one water H atom was calculated based on hydrogen-bonding interactions. The remaining H-atom positions were calculated and treated with a riding model; isotropic displacement parameters were defined as aU_{eq} of the adjacent atom (a = 1.5 for $-CH_3$, OH, and solvate atoms and 1.2 for all others). The PF_6^- anions show typical disorder in these complexes,

dx.doi.org/10.1021/ic202462a | *Inorg. Chem.* 2012, 51, 4572−4587

Scheme 3. Synthesis of Pt(diimine)(pipNHC)Cl^{+a}

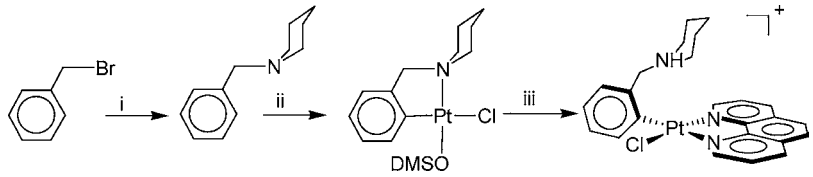

[a](i) Piperidine/benzene; reflux; (ii) $Pt(DMSO)_2Cl_2$, $NaOAC/CH_3OH$; (iii) TFA, 1,10-phenanthroline, KCl/CH_3CN.

which was described with two- or three-component disorder models when possible. In several cases, it was necessary to apply bond restraints or constrain the displacement parameters to keep the anion at a reasonable geometry.

For crystals containing $Pt(phen)(pip_2NCNH_2)(OCN)^{2+}$, the structure was refined with both an OCN group and a Cl atom bonded to the Pt atom with occupancies of 75% and 25%, respectively, giving the most reasonable anisotropic displacement parameters, bond distances, and bond angles. Attempts at modeling the −OCN group such that the N atom is bonded to Pt resulted in very unfavorable anisotropic displacement parameters, bond distances, and bond angles. For crystals containing $Pt(phen)(pip_2NCNH_2)I^{2+}$, a suitable multicomponent disorder model for a few of the C atoms in one of the piperidinium groups was not realized. In crystals with fractional solvate, the solvate was disordered, and restraints were used in some cases.

RESULTS AND DISCUSSION

Synthesis. The rational design and synthesis of square-planar metal complexes with more than four nucleophiles capable of interacting with the metal center is facilitated by using protonation to protect the more basic dangling groups and prevent the formation of a coordinate bond. Scheme 2 shows an efficient synthetic route to arylplatinum(II) complexes, $Pt(diimine)(pip_2NCNH_2)(L)^{2+}$, with a chelating diimine ligand (phen, NO_2phen, or dtfmbpy), a monodentate anionic ligand (L = Cl, Br, I, NCS, NO_2, or OCN), and two dangling protonated piperidyl groups. The chloride ligand was removed from $Pt(pip_2NCN)Cl$ by reaction with $AgPF_6$. A subsequent reaction with the diimine and KL in the presence of trifluoroacetic acid gave $[Pt(diimine)(pip_2NCNH_2)(L)](PF_6)_2$ in 50−70% yield. Excess KSCN and KI were avoided in order to prevent the formation of $Pt(diimine)(SCN)_2$ and $Pt(diimine)I_2$, respectively. In order to synthesize a complex with one dangling piperidinium group using the $pipNC^-$ ligand, we sought to prepare a precursor complex with a single chelating $pipNC^-$ ligand. Reactions of the $pipNC^-$ ligand with $Pt(COD)Cl_2$ proved unsuccessful, resulting in the formation of $Pt(pipNC)_2$, which appears to be a thermodynamic sink in this chemistry.[29] In an alternative approach, $Pt(DMSO)_2Cl_2$, pipNCH, and sodium acetate were refluxed in methanol for 4 h to yield Pt(pipNC)(DMSO)Cl. Treatment with $AgBF_4$ and the subsequent reaction with phen and KCl under acidic conditions gave **9** in ∼50% yield (Scheme 3).

The products were characterized using ^{1}H NMR spectroscopy, MS, and X-ray crystallography. The protonated complexes are stable in an acetonitrile solution and can be treated with 2 equiv of base to give deprotonated adducts. The latter are stable in methylene chloride but gradually decompose in acetonitrile to give the respective $Pt(pip_2NCN)L^{n+}$ complexes (L = halide/pseudohalide or solvent).

^{1}H NMR Spectroscopy. The room-temperature ^{1}H NMR spectra of the diprotonated complexes with phenanthrolinyl ligands in CD_3CN and CD_2Cl_2 solutions show the expected pattern of resonances. Notably, for each complex, one set of diimine resonances and two phenyl proton resonances (in an intensity ratio of 2:1) are observed in the aromatic region. For example, in CD_3CN, the benzylic proton resonances appear in an AX pattern near 4.2 and 4.9 ppm, establishing that these protons are diastereotopic and that coupling to the amine proton is weak, as noted for related systems.[29] For each complex, the chemical shift difference between the benzylic proton resonances is 0.7−0.8 ppm (except for the iodide complex, where it is 0.4 ppm), suggesting significantly different chemical environments. For the series of complexes, the α-piperidinium protons give rise to four resonances with equal intensities from 2.8 to 3.7 ppm; the β- and γ-proton resonances overlap with the solvent and water signals in most cases. Taken together, these data confirm that the combination of inversion about the piperidyl N atom and inversion of the piperidyl ring is slow on the NMR time scale, as expected for a protonated piperidyl group. In addition, asynchronous rotation about the Pt−C bond must also be slow, which is consistent with steric considerations.[29,38−41] Interestingly, the ^{1}H NMR spectra of the $Pt(phen)(pip_2NCNH_2)X^{2+}$ (X = Cl, Br, or I) series reveals that the furthest downfield resonance, assigned to a phen α proton, shifts downfield along the series Cl < Br < I (9.48, 9.68, and 10.03 ppm, respectively), varying linearly with Gutman's donor number for the corresponding halide.[42]

For each complex, the piperidinium NH protons give rise to a broadened resonance in the 7.4−8.2 ppm range. The chemical shifts are similar to those observed for $Pt(diimine)(pipNHC)_2^{2+}$ complexes, which show evidence of NH···Pt hydrogen bonding in solution and the solid state.[29] On the other hand, this resonance is shifted significantly downfield from that of $Pt(tpy)(pip_2NCNH_2)^{3+}$ (6.88 ppm).[26] The Pt center in the latter complex is expected to be comparatively electron-poor, resulting in weaker interactions with the dangling nucleophilic piperidinium groups. Downfield chemical shifts of amine proton resonances from free ligand values are a signature of NH···Pt hydrogen bonding[43,44] but are by no means conclusive proof thereof.[45] For example, we note that the amine resonance shows no evidence of ^{195}Pt satellites and these NMR data alternatively could be interpreted as being consistent with the notion of NH···L hydrogen bonding involving the halide or pseudohalide group (L^-) that is bonded to the metal. In support of this possibility, we note that in their detailed studies of the zwitterionic compounds A−D depicted in Scheme 4, van Koten and co-workers[46−48] encountered examples of both NH···Pt and NH···Br interactions, where the Br was bonded to the Pt center. In $CDCl_3$, complex A with the rigid protonated naphthyl ligand ($1\text{-}C_{10}H_6N(H)Me_2\text{-}8\text{-}C,H$) exhibited the strongest NH···Pt hydrogen-bonding interactions, characterized by amine ^{1}H NMR resonances near 16 ppm and ^{195}Pt coupling constants, $J(^{195}Pt,^1H)$, in the 150−180 Hz range. Such interactions are sufficient to prevent the oxidative addition of HCl to the bis-chelate parent complex, $Pt(1\text{-}C_{10}H_6NMe_2\text{-}8\text{-}$

dx.doi.org/10.1021/ic202462a | Inorg. Chem. 2012, 51, 4572−4587

Scheme 4. (A) Pt(1-$C_{10}H_6NMe_2$-8-*C*,*N*)(1-$C_{10}H_6NHMe_2$-8-*C*,*H*)X, (B) Pt($C_6H_4CH_2NR_2$)($C_6H_4CH_2NHR_2$)Br (R = Me and Et), and (C and D) Pt[(*R*)-$C_6H_4CH(Me)N(CH_3)_2$][(*R*)-$C_6H_4CH(Me)NH(CH_3)_2$]Br[46,47]

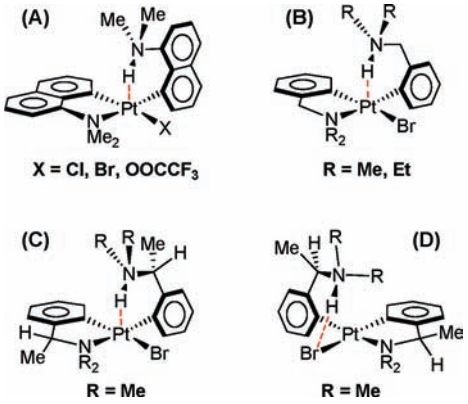

C,*N*)$_2$; on the other hand, CF_3COOH oxidatively adds to form the platinum(IV) hydride as a result of a proposed CF_3COO^- neighboring group effect.[49] In the case of complexes B and C with the less rigid and comparatively flexible benzylic ligand backbone (Scheme 4), the amine resonances are shifted upfield (11−13 ppm) and exhibit smaller coupling constants (66−104 Hz). Two examples of A and B were found to exhibit cross peaks in the 2D ^{1}H NOESY NMR spectra that are consistent with persistent NH···Pt interactions, and $J(^{195}Pt,^1H)$ was proposed to show a correlation with $J(^{15}N,^1H)$ and ν(N−H).[46−48] However, in the case of compound D, which is a conformational isomer of C, steric repulsion between the benzylic methyl group and the −N(CH_3)$_2$ group was proposed to weaken the NH···Pt interaction. Consistent with this conclusion, the amine resonance at 10.9 ppm showed no evidence of ^{195}Pt coupling, which is similar to our observations for the Pt(diimine)(pip_2NCNH_2)X^{2+} series. A crystal structure of D shows the NH group directed toward the middle of the Pt−Br bond, which led those authors to suggest the existence of NH···Br interactions.[46,47] Compared to those zwitterionic complexes, the metal centers in the Pt(diimine)(pip_2NCNH_2)-X^{2+} series are likely to be less basic and form weaker NH···Pt interactions, and therefore NH···L interactions may reasonably be expected to play a comparatively more prominent role.

Interestingly, attempts to prepare [Pt(dtfmbpy)-(pip_2NCNH_2)Cl]$^{2+}$ yielded two products that we were unable to separate. Even ^{1}H NMR spectra of dissolved crystals of **8** show two sets of resonances consistent with two similar products. The aromatic and piperidyl resonances of two species appear as very closely overlapping resonances. There are two sets of benzylic proton resonances appearing as AX patterns near 4.6 and 4.3 ppm, respectively, in a 3:2 intensity ratio. By contrast, the crystal structure shows a single isomer (vide infra), and the MS spectrum is dominated by two fragment peaks consistent with [Pt(dtfmbpy)(pip_2NCNH_2)Cl](PF_6)$^+$ and [Pt(dtfmbpy)(pip_2NCNH_2)Cl]$^{2+}$.

The deprotonated Pt(phen)(pip_2NCN)(L) complexes were prepared in situ by the addition of 2 equiv of base. For example, the addition of 2 equiv of TBAOH to a solution of [Pt(phen)(pip_2NCNH_2)Cl]$^{2+}$ in CD_3CN causes the piperdinium proton resonance to disappear. In freshly prepared solutions, there is no evidence of a free phen ligand or Pt(pip_2NCN)Cl, which is consistent with the diimine ligand remaining bonded to Pt. The benzylic resonances appear as a broad singlet at 4.32 ppm, which is suggestive of monodentate pip_2NCN^- and comparatively rapid rotation about the Pt−C bond. Upon standing, the Pt(phen)(pip_2NCN)Cl resonances gradually lose intensity, while new resonances associated with Pt(pip_2NCN)Cl and phen gain intensity, indicating that the deprotonated product is unstable. Under typical conditions (~1.0 mM), the first-order rate constant is in the (2−4) × 10^{-4} s^{-1} range, which is somewhat less than that found for the Pt(phen)($pipNC)_2$ analogue (10^{-3} s^{-1}) but slightly greater than that of Pt(tpy)(pip_2NCN)$^+$ (10^{-4} s^{-1}). Thus, the stability for this series of complexes, namely, Pt(phen)($pipNC)_2$, Pt(phen)(pip_2NCN)Cl, and Pt(tpy)(pip_2NCN)$^+$ (Scheme 1), increases with increasing rigidity of the ligand framework.

Crystal Structures. The structures of eight diprotonated complexes, Pt(phen)(pip_2NCNH_2)$(L)^{2+}$ (L = Cl, Br, I, NCS, NO_2, or OCN), Pt(dtfmbpy)(pip_2NCNH_2)Cl^{2+}, and Pt-(NO_2phen)(pip_2NCNH_2)Cl^+, and one monoprotonated complex, Pt(phen)(pipNHC)Cl^+, were confirmed by X-ray crystallography (Figure 1 and Tables 1−4). The structure of **1** was determined for crystals without and with solvate (**1**·0.25CH_3CN·0.5H_2O; Figure S1 in the Supporting Information). An attempt to grow crystals of the cyanate complex, Pt(phen)(pip_2NCNH_2)$(OCN)^{2+}$, yielded a crystal whose diffraction pattern was best modeled as Pt(phen)-(pip_2NCNH_2)$(L)^{2+}$ (L = OCN or Cl) with occupancies of 75% and 25% for O-bonded OCN and Cl, respectively. To our knowledge, this is the first example of a structurally characterized platinum(II) O-bonded cyanate complex. It should be noted that the NH piperidinium and water solvate H atoms were located directly from the difference maps. The one exception is **1**·0.25CH_3CN·0.5H_2O, for which the position of one water H atom was calculated based on hydrogen-bonding interactions. The positions of all other H atoms were calculated. In each case, the molecules pack as discrete units, and there are no unusually short interionic interactions. However, in crystals containing Pt(phen)(pip_2NCNH_2)-(NCS)$^{2+}$, the water solvate participates in hydrogen bonds with one protonated piperidyl group [N4···O1W = 2.794(4) Å] and the acetonitrile solvate [OW1···N7 = 2.847(5) Å; Figure S1 in the Supporting Information]. In crystals of **1**·0.25CH_3CN·0.5H_2O, the water solvate forms a short hydrogen bond with the chloro ligand [O1···Cl = 2.419(6) Å; Figure S1 in the Supporting Information] and a longer interaction with the acetonitrile solvate [O1···N5 = 2.886(24) Å]. On the other hand, for [Pt(NO_2phen)(pip_2NCNH_2)Cl]$^{2+}$, the −OH group of methanol solvate forms a weak interaction with the chloro ligand [O1S···Cl = 3.675(1) Å; Figure S1 in the Supporting Information].

For each complex, the coordination geometry is approximately square-planar, with N−Pt−L and N−Pt−C bond angles [171.5(1)−177.2(4)°] similar to those reported for Pt-(diimine)$(pipNHC)_2^{2+}$ complexes [171.4(2)−174.3(1)°].[29] Overall, the bond lengths and angles of the cations of the chloro complexes are similar to those of Pt(2,2′-bpy)(*p*-tolyl)Cl.[50] For each complex, the coordination plane (defined by the four atoms bonded to Pt) shows a small tetrahedral distortion. The largest root-mean-square deviations for the diprotonated series are for the two complexes in the asymmetric unit of the Pt(phen)(pip_2NCNH_2)I^{2+} salt (0.0742 and 0.0509 Å). The N2−Pt−L angles [96.46(13) and 96.62(13)°] also are slightly greater than those for the other salts [92.9(4)−95.59(6)°, except the nitrito complex, which

dx.doi.org/10.1021/ic202462a | *Inorg. Chem.* 2012, 51, 4572−4587

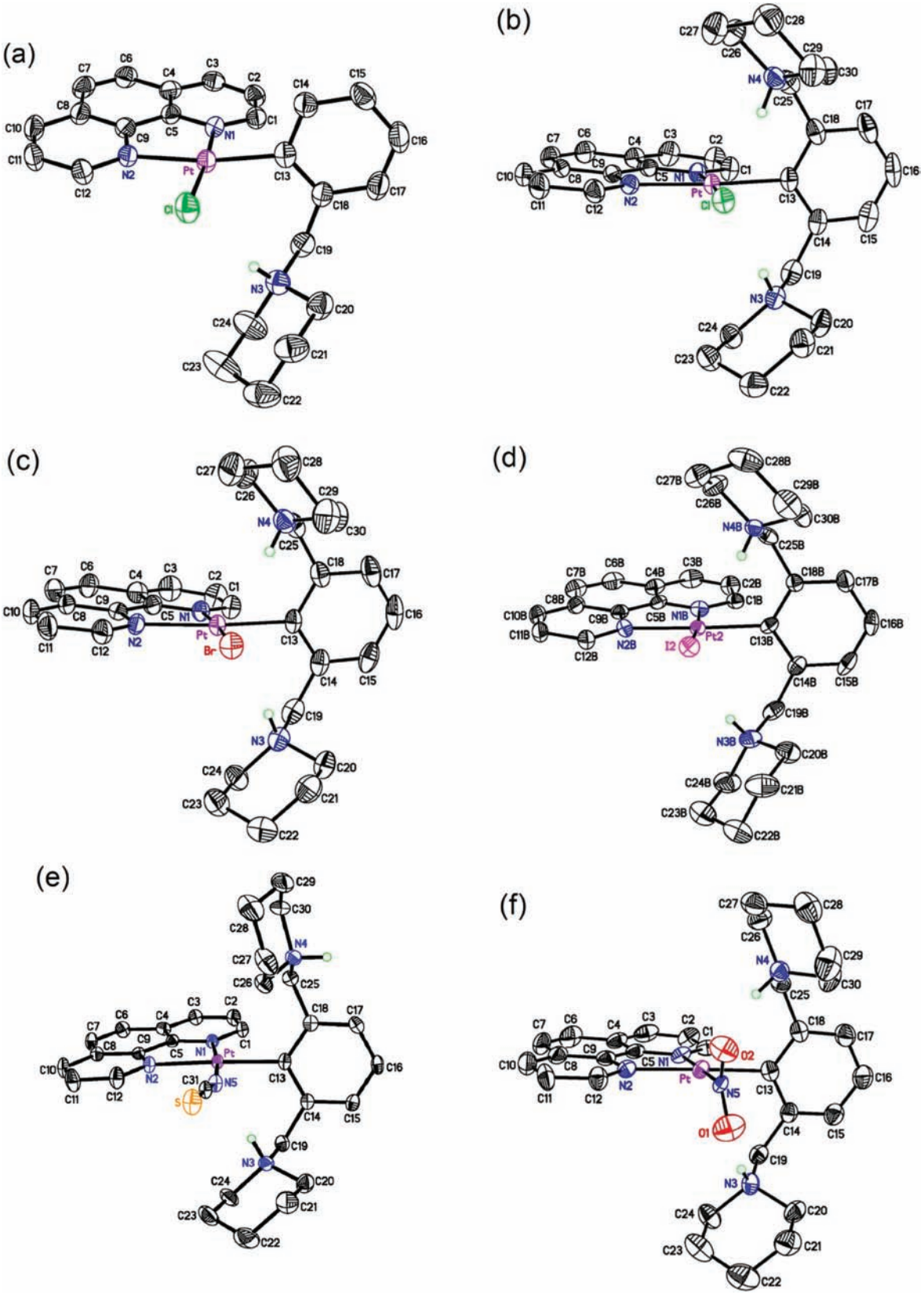

Figure 1. continued

dx.doi.org/10.1021/ic202462a | *Inorg. Chem.* 2012, 51, 4572−4587

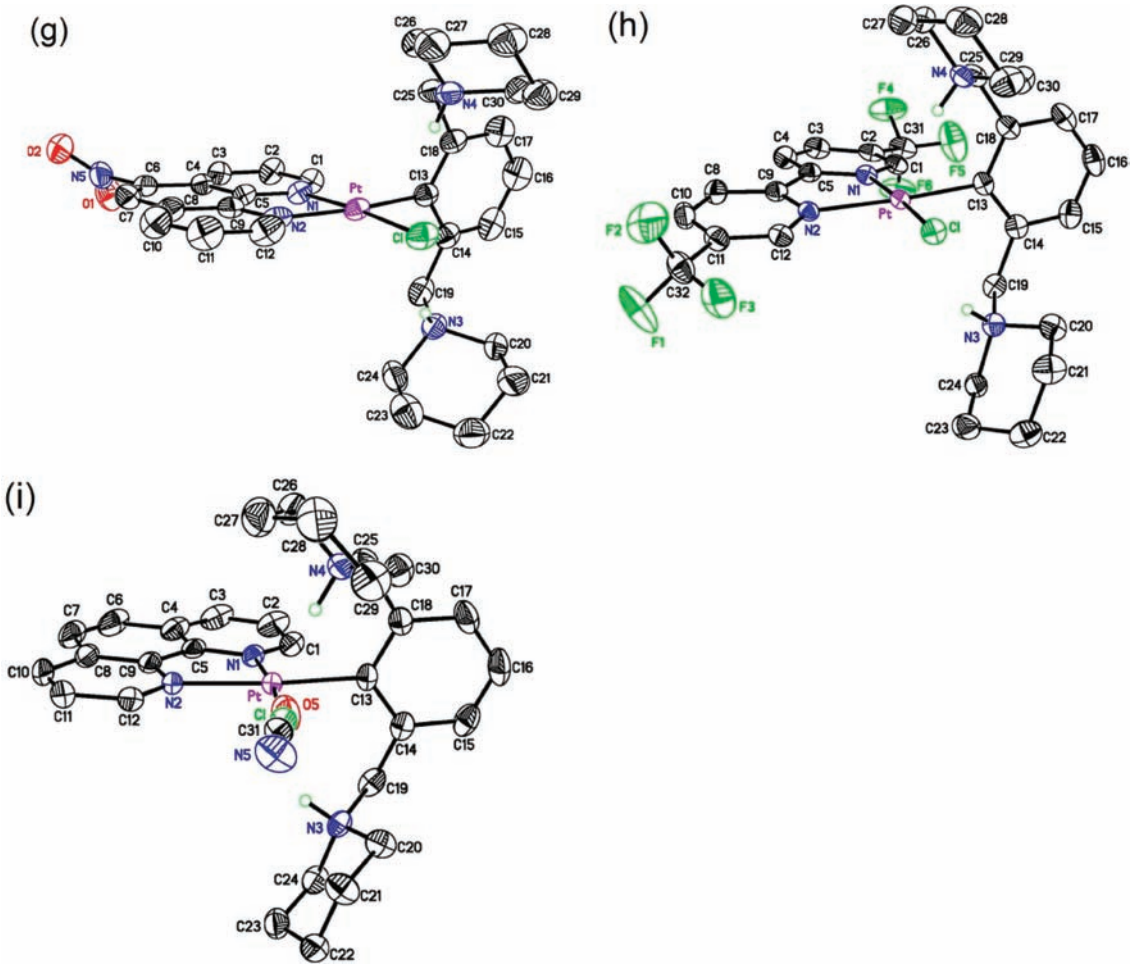

Figure 1. ORTEP drawings of cations in (a) **9**·CH_3CN, (b) **1**, (c) **2**, (d) **3**, one of two independent molecules shown, (e) **4**·CH_3CN·H_2O, (f) **5**·CH_3CN, (g) **7**·0.25CH_3OH, (h) **8**, and (i) $(\mathbf{1})_{0.25}(\mathbf{6})_{0.75}$·0.5$CH_3CN$. Anions, solvent, and H atoms [with the exception of those bonded to N(piperidyl)] are omitted for clarity (50% probability ellipsoids).

Table 1. Crystal and Structure Refinement Data

	1	1·0.25CH_3CN·0.5H_2O	$(\mathbf{1})_{0.25}(\mathbf{6})_{0.75}$·0.5$CH_3CN$	2	3
formula	$[C_{30}H_{37}N_4ClPt](PF_6)_2$	$[C_{30}H_{37}N_4ClPt](PF_6)_2$·0.25$CH_3CN$·0.5$H_2O$	0.75{$[C_{31}H_{37}N_5OPt](PF_6)_2$} + 0.25{$[C_{30}H_{37}N_4ClPt](PF_6)_2$}·0.5$CH_3CN$	$[C_{30}H_{37}N_4BrPt](PF_6)_2$	$[C_{30}H_{37}N_4IPt](PF_6)_2$
T, K	173(2)	173(2)	150(2)	173(2)	150(2)
cryst syst	monoclinic	monoclinic	monoclinic	monoclinic	orthorhombic
space group	$C2/c$	$P2/c$	$P2/c$	$C2/c$	$Pca2_1$
a, Å	23.6176(18)	12.9652(8)	12.9207(4)	23.9210(19)	24.886(3)
b, Å	10.6519(8)	12.1867(8)	12.2183(4)	10.7075(8)	8.0909(10)
c, Å	27.906(2)	24.3433(15)	24.2249(8)	27.772(2)	35.751(5)
α, deg	90	90	90	90	90
β, deg	98.797(2)	102.276(1)	102.173(2)	98.747(2)	90
γ, deg	90	90	90	90	90
R1/wR2 [$I > 2\sigma(I)$]	0.0302/0.0788	0.0346/0.0926	0.0343/0.0937	0.0351/0.0985	0.0375/0.0873
R1/wR2 (all data)	0.0328/0.0807	0.0401/0.0959	0.0353/0.0946	0.0370/0.1000	0.0403/0.0886

was 96.5(2)°], which is suggestive of steric repulsion between the I atom and nearby phen α-H atom. In each structure, the aryl group accommodates the chelating diimine ligand by rotation about the Pt−C bond, resulting in a dihedral angle with the coordination plane in a narrow range [NCS^-, 76.0(1)°; all others, 84.7(1)−88.4(1)°]. Hydrogen bonding of a piperidinium group with solvate in the Pt(phen)-$(pip_2NCNH_2)(NCS)^{2+}$ salt causes the aryl group to be rotated less. The Pt−N2(diimine) distances trans to the phenyl ring [2.088(2)−2.113(5) Å] are very similar to those found for Pt(diimine)$(pipNHC)_2^{2+}$ complexes[29] and fall within the range observed for related complexes with aryl groups trans to diimine ligands (2.08−2.12 Å).[51−55] The Pt−N1 distances are shorter [2.005(3)−2.043(5) Å], in accordance with the relative trans influence of the halide/pseudohalide ligands. The Pt−N1 distances for the Pt(phen)$(pip_2NCNH_2)(L)^{2+}$ structures follow

dx.doi.org/10.1021/ic202462a | Inorg. Chem. 2012, 51, 4572−4587

Table 2. Crystal and Structure Refinement Data

	4·2CH_3CN·H_2O	5·CH_3CN	7·0.25CH_3OH	8	9·CH_3CN
formula	$[C_{31}H_{37}N_5SPt](PF_6)_2$·2$CH_3CN$·$H_2O$	$[C_{30}H_{37}N_5O_2Pt](PF_6)_2$·$CH_3CN$	$[C_{30}H_{36}N_5O_2ClPt](PF_6)_2$·0.25$CH_3OH$	$[C_{30}H_{35}N_4F_6ClPt](PF_6)_2$	$[C_{24}H_{25}N_3ClPt]BF_4$·$CH_3CN$
T, K	150(2)	150(2)	193(2)	150(2)	193(2)
cryst syst	triclinic	orthorhombic	triclinic	monoclinic	monoclinic
space group	$P\bar{1}$	$Pna2_1$	$P\bar{1}$	$P2_1/c$	$P2_1/c$
a, Å	10.5437(3)	16.174(3)	9.2003(6)	12.3801(4)	9.3658(7)
b, Å	14.7258(4)	18.447(3)	13.1174(9)	12.4952(4)	26.227(2)
c, Å	16.3354(5)	12.683(2)	16.0170(11)	24.1575(8)	11.0318(9)
α, deg	63.216(1)	90	86.300(1)	90	90
β, deg	71.705(1)	90	79.461(1)	96.102(1)	104.003(2)
γ, deg	69.919(1)	90	72.667(1)	90	90
R1/wR2 [$I > 2\sigma(I)$]	0.0248/0.0615	0.0370/0.0905	0.0577/0.1546	0.0218/0.0535	0.0246/0.0621
R1/wR2 (all data)	0.0263/0.0625	0.0399/0.0921	0.0587/0.1560	0.0234/0.0544	0.0303/0.0642

Table 3. Selected Distances for 1−3 (Å)

	1	1·0.25CH_3CN·0.5H_2O	$(1)_{0.25}(6)_{0.75}$·0.5CH_3CN	2	3
Pt−C13	2.014(3)	2.028(4)	2.031(4)	2.020(4)	1.994(6), 2.014(6)
Pt−N1	2.005(3)	2.011(4)	2.008(4)	2.019(3)	2.043(5), 2.025(5)
Pt−N2	2.103(3)	2.101(4)	2.101(4)	2.105(3)	2.113(5), 2.113(5)
Pt−L	2.3103(8)	2.3468(15)	2.110(16), 2.236(13)	2.4247(4)	2.5996(5), 2.6022(5)
H3···L	2.51	2.77	2.79, 2.78	2.58	2.73, 2.84
N3−L	3.360(3)	3.516(4)	3.474(16), 3.472(11)	3.476(3)	3.582(5), 3.663(5)
H3···Pt	2.75	2.62	2.58	2.71	3.28, 2.82
N3···Pt	3.335(3)	3.352(4)	3.329(4)	3.357(4)	3.722(5), 3.458(5)
H4···L	2.35	2.44	2.16, 2.30	2.49	2.84, 2.75
N4−L	3.254(3)	3.304(4)	3.124(17)	3.357(3)	3.673(5), 3.594(5)
H4···Pt	2.85	2.78	2.62	3.02	2.52, 3.30
N4···Pt	3.486(3)	3.417(4)	3.393(4)	3.535(4)	3.384(5), 3.750(5)

Table 4. Selected Distances for 4−8 (Å)

	4·2CH_3CN.H_2O	5·CH_3CN	7·0.25CH_3OH	8	9·CH_3CN
Pt−C13	2.031(3)	2.021(6)	2.035(5)	2.024(3)	2.012(3)
Pt−N1	2.022(2)	2.022(4)	2.026(4)	2.021(2)	2.008(3)
Pt−N2	2.088(2)	2.098(5)	2.107(5)	2.108(2)	2.107(2)
Pt−L	2.008(3)	2.061(4)	2.3157(13)	2.3019(6)	2.3130(8)
H3···L	2.03	2.68	2.58	2.47	2.36
N3−L	2.976(4)	3.490(7)	3.374(5)	3.342(2)	3.228(3)
H3···Pt	2.84	3.10	2.86	2.94	3.02
N3···Pt	3.502(3)	3.517(4)	3.395(4)	3.560(2)	3.538(3)
H4···L		2.62	2.45	2.62	
N4−L		3.467(6)	3.230(4)	3.431(2)	
H4···Pt		2.98	2.78	2.71	
N4···Pt		3.700(4)	3.466(4)	3.389(2)	

the trend Cl < Br < NCS ≈ NO_2 < I [L, d_{Pt-N1}: Cl, 2.005(3) for **1** and 2.011(4) for **1**·0.25CH_3CN·0.5H_2O; Br, 2.019(3); I, 2.025(5) and 2.043(5); NCS, 2.022(2); NO_2, 2.022(4)]. The Pt−L distances are normal,[56−62] except that the Pt−Cl bond is elongated for the structure in which the chloro ligand forms a hydrogen bond with water solvate [2.3468(15) vs 2.3019(6)−2.3157(13) Å for the other chloro structures, except the disordered cyanate structure]. The Pt−C distances [1.994(6)−2.035(5) Å] are within the range observed for Pt(pip_2NCN)(L)$^+$ complexes with pyridyl groups positioned trans to the aryl ligand (1.91−2.04 Å).[26,27,35,51,63,64]

In nearly every structure, both of the piperidinium NH groups are directed approximately toward the coordination plane, resulting in short contacts to the metal-bonded halide or pseudohalide ligand (NH···L for 20 measurements: 2.03−2.84 Å). These interactions are emphasized in Figures 2 and S2 in the Supporting Information. The lone exception is Pt(phen)(pip_2NCNH_2)(NCS)$^{2+}$, in which one of the protonated piperidyl groups forms a hydrogen bond with water solvate, as mentioned previously. In nearly all instances, the NH···L distances also are *less than* the sum of the van der Waals radii.[65,66] One exception is Pt(phen)(pip_2NCNH_2)(NO_2)$^{2+}$, in which there are, instead, very short NH···O contacts involving the nitrite O atoms [N···O = 2.808(7) and 2.891(6) Å; NH···O = 1.91−2.06 Å] and the NO_2^- group forms a 83.2(2)° dihedral angle with the coordination plane (Figure S2 in the Supporting Information). The other exception is for one of the piperidinium groups in the disordered cyanate complex

dx.doi.org/10.1021/ic202462a | Inorg. Chem. 2012, 51, 4572−4587

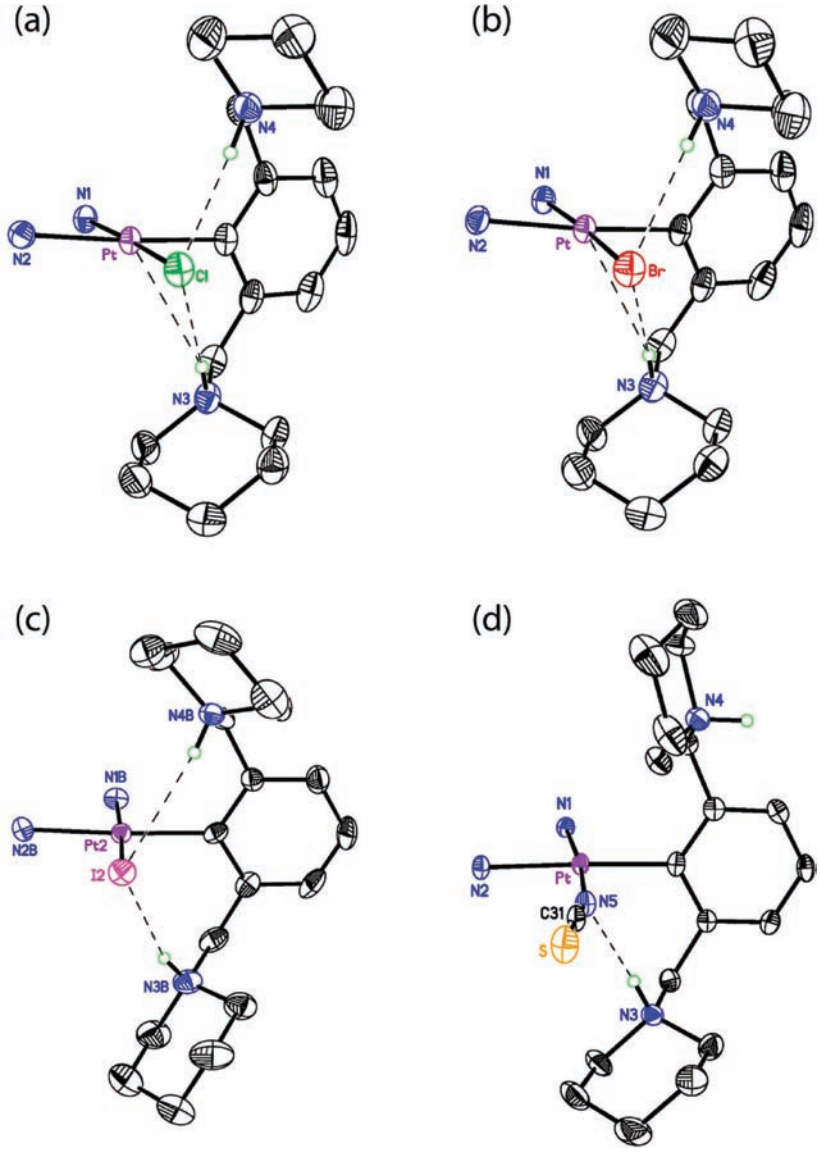

Figure 2. ORTEP drawings of cations showing the NH···L and NH···Pt interactions (dashed lines) that are less than the sum of the van der Waals radii for (a) **1**, (b) **2**, (c) molecule B in **3**, and (d) **4**·CH_3CN·H_2O. Anions, solvent, C atoms of the diimine ligand, and H atoms [with the exception of those bonded to N(piperidyl)] are omitted for clarity (50% probability ellipsoids).

[N3···O5 = 3.474(16)Å; H3···O5 = 2.79 Å]. For each complex, the orientation of the NH groups also results in short NH···Pt distances (2.52−3.30 Å). About half of these distances (11 of 20) are less than the sum of the van der Waals radii. Additionally, the NH···Pt (110−147°) and NH···L (132−178°) bond angles are consistent with hydrogen bonding. The connection between the NH···Pt distance and the N−H···Pt angle is suggested by an approximate linear relationship (r^2= 0.70; Figure 3a). A similar relationship exists between the N−H···L angle and the difference between the NH···L distance (d_{H-L}) and the van der Waals radius ($r_{vdw(L)}$) of the metal-bonded atom of the halide or pseudohalide ligand (L^-; r^2 = 0.61; Figure 3b).

For the purposes of comparison, we consider the structures of four previously investigated Pt(diimine)$(pipNHC)_2^{2+}$ complexes with short NH···Pt contacts (2.32−2.51 Å) and N−H···Pt angles in the 141−155° range, suggesting NH···Pt hydrogen bonding.[29] For those systems, it was proposed that the geometric constraints of the pipNHC ligand prevent a more linear NH···Pt arrangement, which would be more optimal for a dipole−monopole interaction. We believe that similar constraints exist for the systems presented here. However, it is apparent that the NH···Pt interactions are longer for Pt(diimine)$(pip_2NCNH_2)(L)^{2+}$, presumably because of competition from the halide/pseudohalide ligand. Moreover, the NH···L interactions appear to be stronger than the NH···Pt interactions, as suggested by the relative values of the N−H···L and N−H···Pt angles. [For the purposes of this discussion, values for Pt(phen)$(pip_2NCNH_2)Cl^{2+}$ derived from the structure of the disordered cyanate complex are excluded.] In addition, each of the NH···Pt distances and half of the NH···L interactions (10 of 20) exceed the distance between the piperidinium proton and the Pt−L bond centroid by ≥0.1 Å. Thus, the NH groups have the appearance of being directed more toward the L atom or Pt−L bond rather than toward the Pt atom. Although the proton-acceptor properties of metal-bonded halides[46,47] and Pt^{II} centers are well documented,[29,43,45−47,67−70] we know of only one structurally

dx.doi.org/10.1021/ic202462a | Inorg. Chem. 2012, 51, 4572−4587

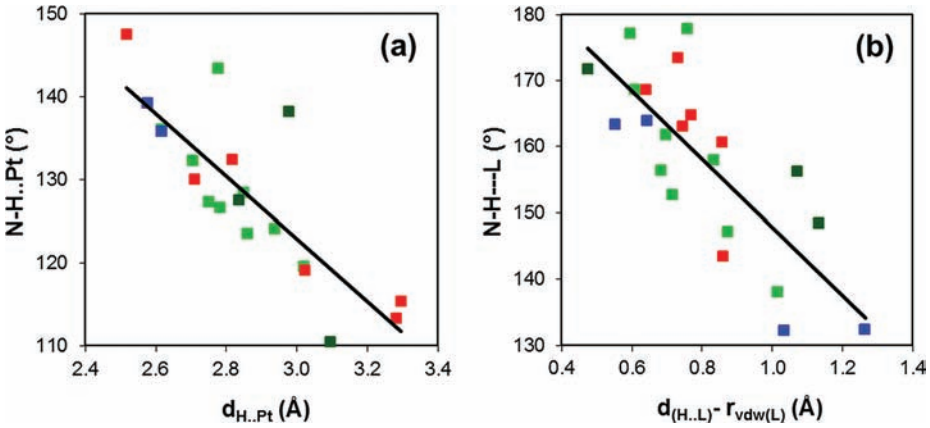

Figure 3. (a) N−H···Pt angle versus H···Pt distance: (light-green) chloro, (red) bromo and iodo, (blue) isocyanato, (dark-green) nitrito and isothiocyanato, (solid line) linear fit to all data points [$y = 235.9-37.7(d_{(H-Pt)})$; $r^2 = 0.70$]. (b) N−H···Pt angle versus the difference between the H···L distance ($d_{(H-L)}$) and the van der Waals radius ($r_{vdw(L)}$) of the metal-bonded atom of the halide or pseudohalide ligand: (light-green) chloro, (red) bromo and iodo, (blue) isocyanato, (dark-green) nitrito and isothiocyanato, (solid line) linear fit to all data points ($y = -51.6x + 199.4(d_{(H-L)} - r_{vdw(L)})$; $r^2 = 0.61$).

characterized example in which the orientation of the N−H vector is directed toward a Pt−L bond, namely, compound D depicted in Scheme 4.[46,47] In that case, steric repulsion between the benzylic methyl group and the $-N(CH_3)_2$ group was proposed to account for weakening of the NH···Pt interaction. By contrast, for the series of structures reported here, there are no obvious steric constraints favoring the observed orientation of the N−H vector. Notably, even for the iodo complex, which has the shortest NH···Pt contact (Figure S2b in the Supporting Information), there is no evidence of increased steric congestion. Moreover, the wide range of NH···Pt distances (2.52−3.30 Å) and N−H···Pt angles (113.0−153.4°) also suggests that steric/conformational factors are not overriding.

To understand the conformational changes contributing to the variation in the NH···Pt contacts and N−H···Pt angles, we have analyzed the structural variations in the 6-atom [···Pt−C−C−C−N−H···] ring. To a good approximation, the Pt−C−C−C fragment is planar, which reduces the dependence of the NH···Pt distance to 11 conventional parameters (five bond distances, four bond angles, and two bond torsion angles). Accordingly, the calculated NH···Pt distances and N−H···Pt angles based on these measured parameters are strongly correlated with the experimental values (r^2 = 0.94 and 0.98, respectively; Figure S3 in the Supporting Information). The experimental C−N−H angle and C−C−C−N torsion angle are by far the most important parameters, and using average values for all of the others still gives very good agreement between the calculated and experimental values (r^2: NH···Pt distances, 0.85; N−H···Pt angles, 0.90; Figure S4 in the Supporting Information). The importance of the C−N−H bond angle is consistent with the rather wide variation in the experimental values [average of 19 angles: 107(7)°]. The importance of rotation about the benzylic C−C bond compared to rotation about the C−N bond can be understood in terms of the arcs swept out by the H atom upon rotation. The average radius for the C−C rotation [1.95(8) Å] is more than twice that for the C−N rotation [0.86(6) Å]. Additionally, the angle between the Pt···H vector and a tangent to the arc of rotation at the H atom tends to be greater for the benzylic C−C rotation [125(3) vs 100(11)°], making the Pt···H distance more sensitive to rotation about the C−C bond.

We were especially interested in assessing the influence of the electronic properties of the halide/pseudohalide ligand on the NH···L/NH···Pt interactions. For this purpose, we define $\gamma = a + b$ as a measure of the combined NH···L and NH···Pt interactions involving one piperidinium group, where r(H···L) and r(H···Pt) are interatomic distances, r_H, r_{Pt}, and r_L are van der Waals radii, and

$$a = \begin{cases} 0 \text{ if } r(\text{H}\cdots\text{Pt}) \geq r_H + r_{Pt} \\ r(\text{H}\cdots\text{Pt}) - r_H - r_{Pt} \text{ if } r(\text{H}\cdots\text{Pt}) < r_H + r_{Pt} \end{cases}$$

$$b = \begin{cases} 0 \text{ if } r(\text{H}\cdots\text{L}) \geq r_H + r_L \\ r(\text{H}\cdots\text{L}) - r_H - r_L \text{ if } r(\text{H}\cdots\text{L}) < r_H + r_L \end{cases}$$

Values of γ for 18 measurements range from −0.23 to −0.64 Å; values for the NO_2^- complex (0.00, −0.02 Å) were excluded because the N−H bond vectors are directed toward the nitrite O atoms. Values of less than zero are indicative of significant NH···L/NH···Pt interactions. For the complexes with thiocyanate (γ = −0.62 Å) and pipNHC (γ = −0.48 Å) ligands, only one piperidinium group interacts with Pt/L. Values of γ for these complexes are among the smallest, which is consistent with a tendency for the removal of one piperidinium group to be compensated for by strengthening the interactions with the piperidinium group on the opposite face. For example, the cyanate adduct has widely disparate values (−0.23, −0.64 Å). Thus, the average of γ ($\langle\gamma\rangle$) for the seven structures having two interacting piperidinium groups falls within a very narrow range (−0.35 to −0.48 Å). Interestingly, whereas $\langle\gamma\rangle$ varies only modestly, the average N−H···X angle decreases along the chloro (−0.44 Å, 177°), bromo (−0.45 Å, 171°), and iodo (−0.44 Å, 158°) series of $Pt(phen)(pip_2NCNH_2)(X)^{2+}$ complexes, in accordance with the relative gas-phase proton affinities of the halides. It also has not escaped our notice that $\langle\gamma\rangle$ is larger and the average N−H···X angle $\langle\theta\rangle$ is smaller for the chloro adducts with more weakly donating diimine ligands (NO_2phen, −0.35 Å, 160°; dtfmbpy, −0.35 Å, 150°), as might be expected for the reduced basicity of the Pt−L unit. Similarly, $\langle\gamma\rangle$ is larger (and $\langle\theta\rangle$ is smaller) for the adduct in which the chloro group is hydrogen bonding with water solvate (−0.35 Å, 147° vs −0.44 Å, 177°). The accumulated observations are consistent with the notion that increasing the electron density

dx.doi.org/10.1021/ic202462a | Inorg. Chem. 2012, 51, 4572−4587

on the metal center tends to enhance the NH···L/NH···Pt interactions. It is apparent that these interactions are comparable in strength to hydrogen bonds and that a competing intramolecular hydrogen-bonding interaction can effectively peel one of the piperidinium groups away from the Pt−L unit, as in the case of the thiocyanate adduct. However, as is found in structures of related Pt(diimine)$(pipNHC)_2^{2+}$ salts,[29] in no instances are both piperidinium groups found to interact with a basic solvate molecule or counteranion.

Electronic and Emission Spectroscopy. In order to assess the influence of the dangling piperidyl and piperidinium groups on the electronic structures of these complexes, electronic absorption and emission spectra were recorded. The yellow Pt(diimine)$(pip_2NCNH_2)(L)^+$ salts dissolve in CH_2Cl_2 to give yellow solutions. In keeping with the absorption spectra of related platinum(II) complexes, an intense phen ligand-localized (^{1}LL) transition occurs near 275 nm.[71,72] At longer wavelengths, two distinct maxima occur in the 340−380 nm range, having spacings consistent with vibronic structure (Table 5). A survey of the spectra of related complexes suggests

Table 5. UV−Visible Absorption Spectroscopy Data in CH_2Cl_2

compound	wavelength (nm) (ε, 10^4 M^{-1} cm^{-1})
[Pt(phen)$(pip_2NCNH_2)Cl](PF_6)_2$ (**1**)	278 (2.97), 305sh (1.07), 332sh (0.42), 348 (0.35), 366 (0.34)
Pt(phen)$(pip_2NCN)Cl$	264 (2.85), 273 (2.95), 328sh (0.47), 378 (0.32)
[Pt(phen)$(pip_2NCNH_2)Br](PF_6)_2$ (**2**)	278 (3.23), 305sh (1.07), 333sh (0.42), 350 (0.36), 367 (0.36)
Pt(phen)$(pip_2NCN)Br$	261(2.6), 276(2.83), 326sh (0.50), 378 (0.32)
[Pt(phen)$(pip_2NCNH_2)I](PF_6)_2$ (**3**)	279 (3.05), 300sh (1.16), 357sh (0.33), 370 (0.35)
Pt(phen)$(pip_2NCN)I$	265 (3.2), 278sh (2.2), 363 (0.35), 438 (0.24), 500sh (0.10)
[Pt(phen)$(pip_2NCNH_2)(NCS)](PF_6)_2$ (**4**)	279 (2.89), 305sh (1.04), 351 (0.36), 368 (0.38)
Pt(phen)$(pip_2NCN)(NCS)$	268 (2.61), 297sh (1.06), 359 (0.37), 416 (0.26), 500sh (0.05)
[Pt(phen)$(pip_2NCNH_2)(NO_2)](PF_6)_2$ (**5**)	278 (2.97), 305 (0.92), 341 (0.28), 358 (0.23)
Pt(phen)$(pip_2NCN)(NO_2)$	266 (3.30), 280sh (1.90), 298sh (1.25), 405sh (0.23), 490sh (0.08)
[Pt$(NO_2phen)(pip_2NCNH_2)Cl](PF_6)_2$ (**7**)	282 (1.44), 314sh (0.56), 350sh (0.30), 367sh (0.21)
Pt$(NO_2phen)(pip_2NCN)Cl$	270 (1.57), 317sh (0.51), 400 (0.22)

that moderately intense metal-to-ligand charge-transfer (MLCT) *and* LL transitions can occur in this region. For example, Pt(phen)$(pipNHC)_2^{2+}$ gives rise to two comparably intense solvent-insensitive absorption maxima at 348 nm (3600 M^{-1} cm^{-1}) and 365 nm (3800 M^{-1} cm^{-1}).[29] Although variations in the electron-donor properties of ancillary ligands (L′) of Pt(phen)$(L')_2^{n+}$ can be expected to dramatically perturb the energies of the charge-transfer (CT) states of platinum(II) diimine complexes,[73,74] two similar features appear in the 340−380 nm range in the spectra of a wide array of phen derivatives, regardless of the ancillary ligand.[71,72,75] A notable example is the spectrum of Pt(phen)$_2^{2+}$ (352 and 373 nm), in which the lowest spin-allowed MLCT band is clearly shifted to much shorter wavelengths, yet there remain two distinct maxima near 352 and 373 nm,[72] which we attribute to a LL transition. For the Pt(phen)$(pip_2NCNH_2)(L)^{2+}$ series, the two features undergo a gradual broadening and a slight shift to lower energy along the series NO_2 > Cl > Br > SCN > I (Figure 4a). This order is similar to that found for MLCT transitions of

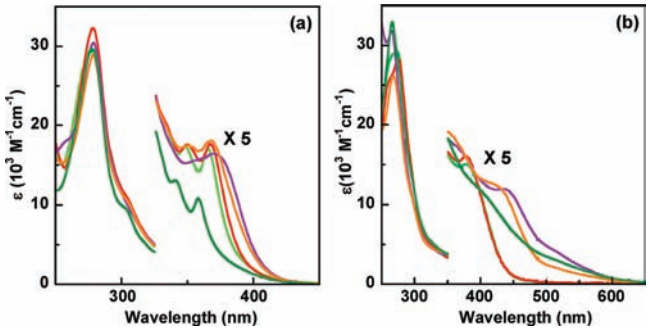

Figure 4. Electronic absorption spectra of (a) Pt(phen)$(pip_2NCNH_2)(L)^{2+}$ in CH_2Cl_2, where L = Cl (light-green line), Br (red line), I (purple line), NCS (orange line), and NO_2 (dark-green line), and (b) after the addition of 2 equiv of base in CH_2Cl_2, where L = Cl (light-green line), Br (red line), I (purple line), NCS (orange line), and NO_2 (dark-green line).

Ru(diimine)$_2L_2$ complexes in acetonitrile (NO_2 > SCN > Cl > Br > I).[76] The slight difference in ordering is likely related to the fact that the overall shift for the platinum(II) series is substantially smaller (~600 cm^{-1}) than that for the ruthenium(II) series (~3000 cm^{-1}). For example, the shift in the absorption band maximum upon substitution of NO_2 for Cl in Pt(diimine)$(pip_2NCNH_2)(L)^{2+}$ (600 cm^{-1}; Figure 4a) is less than half that found for the longest-wavelength spin-allowed MLCT band of Ru(tpy)(bpy)$(L)^+$ (1400 cm^{-1}).[77,78] Both the smaller shift and the broadening along the platinum(II) series are consistent with stabilization of a MLCT state in the vicinity of the LL state, resulting in band overlap and/or MLCT/LL mixing. It is difficult to distinguish between these possibilities at this time.

It is noteworthy that platinum(II) phenanthroline complexes with phenyl donor ligands exhibit MLCT transitions in the 400−500 nm region[79] [e.g., Pt(phen)$(Ph)_2$, CH_2Cl_2, 437 nm][29] and that the longest-wavelength maximum for Pt(phen)Cl_2 occurs at 396 nm, red-shifted by 2100 cm^{-1} from that of Pt(phen)$(pip_2NCNH_2)Cl^{2+}$. The remarkable *destabilization* of MLCT states of Pt(phen)$(pip_2NCNH_2)Cl^{2+}$ is attributable to the interaction of one or both of the piperidinium NH groups with the Pt−Cl unit, which tends to stabilize the metal-centered orbitals. Accordingly, we note that the addition of 2 equiv of TBAOH causes a significant red shift and broadening in the long-wavelength region of the absorption spectrum (Figure 4b). Whereas the longest-wavelength absorption maximum for the diprotonated phen adducts falls within a narrow 900 cm^{-1} range (358−370 nm), a comparably intense feature in the spectra of the deprotonated complexes appears as a maximum or shoulder over a 3600 cm^{-1} range (378−438 nm). This sensitivity to the protonation state is remarkable given that the piperidinium N atoms are four and five covalent bonds removed from the metal center and phenanthrolinyl ligands, respectively. The results are consistent with stabilization of a transition having significant MLCT character, which is expected to occur upon loss of the NH···Pt/L interactions. Similar results have been observed for Pt(phen)$(pipNHC)_2^{2+}$/Pt(phen)$(pipNC)_2$ complexes, in which intramolecular NH···Pt interactions destabilize MLCT states.[29] It is intriguing that the resulting 3600 cm^{-1} range of the 378−438 nm feature for

dx.doi.org/10.1021/ic202462a | *Inorg. Chem.* 2012, 51, 4572−4587

the Pt(phen)(pip$_2$NCN)(L) series exceeds the range observed for Ru(diimine)$_2$L$_2$ complexes with *two* halide/pseudohalide ligands (3000 cm^{-1}).[77,78] Moreover, the energy ordering of these bands in the spectra of the platinum complexes is somewhat different: Cl ≈ Br > NO$_2$ > NCS > I. In the cases of L = NO$_2$, NCS, and I, there is an additional weak, but very broad band near 500 nm (500−1000 M^{-1} cm^{-1}). Spectral changes accompanying the gradual addition of 2 equiv of base to the chloro (phen and NO$_2$phen), bromo, and iodo adducts are consistent with an A → B → C process. For example, titration of a CH_2Cl_2 solution of the bromo adduct results in two sets of sharp isosbestic points (Figure 5). The behavior for

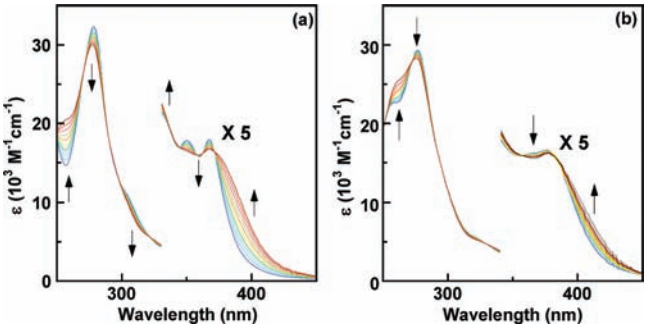

Figure 5. UV−visible absorption spectra recorded during the addition of 100 μM TBAOH to a 50 μM solution of **1** in CH_2Cl_2. The addition of (a) 1 equiv and (b) a second equiv in 0.1 molar increments.

the chloro, bromo, and iodo adducts is consistent with the mono- and diprotonated adducts having different pK_a values. Interestingly, the addition of the first equiv of base has a significantly greater impact on the longest-wavelength absorption features than that of the second equiv. This effect is dramatic in the case of the iodo adduct, in which the first equiv of base shifts the longest-wavelength band by ∼4000 cm^{-1} to near 435 nm, whereas the second equiv only causes broadening of the long-wavelength tail of that band (Figure S6 in the Supporting Information). Taken together with our earlier report,[29] these results demonstrate that electronic spectroscopy is an exceptionally sensitive tool for probing intramolecular NH···Pt and NH···L interactions.

Assignment of the long-wavelength bands in the deprotonated adducts cannot yet be made with certainty. We have observed similar features in the spectra of a series of related platinum(II) complexes with dangling nucleophiles and π-acidic pyridyl ligands,[26,27,80] including Pt(diimine)(pipNC)$_2$ complexes.[29] It can be reasonably expected that the interaction of dangling basic groups at open coordination sites of the metal center will stabilize CT transitions having metal-to-pyridyl ligand character. However, the extent of such interactions (if any) in the Pt(phen)(pip$_2$NCN)(L) series is not currently known. Each diprotonated complex (L = Cl, Br, I, NO$_2$, or NCS) gives rise to intense green emissions in the solid state and in a 77 K frozen solution. However, only Pt(phen)(pip$_2$NCNH$_2$)(NCS)$^{2+}$ is emissive in a fluid solution, exhibiting a weak and broad green emission near 519 nm. In 77 K dilute butyronitrile frozen glassy solutions, each complex gives rise to an intense blue-green emission, originating near 450 nm (Figure S10 in the Supporting Information and Table 6). The structured emission profiles are characteristic of a lowest ^{3}LL excited state.[72,73,81−84] The vibronic structure with 1230−1630 cm^{-1} spacings is consistent with overlapping progressions of

Table 6. Emission Spectroscopic Data in Butyronitrile Solution

compound	conditions	emission maxima (nm)
[Pt(phen)(pip$_2$NCNH$_2$)Cl](PF$_6$)$_2$ (**1**)	77 K, glassy solution	466, 496, 531, 583sh
[Pt(phen)(pip$_2$NCNH$_2$)I](PF$_6$)$_2$ (**3**)	77 K, glassy solution	469, 501, 534, 585sh
[Pt(phen)(pip$_2$NCNH$_2$)(NCS)](PF$_6$)$_2$ (**4**)	77 K, glassy solution	469, 499, 538, 584sh
	room temperature	519
[Pt(phen)(pip$_2$NCNH$_2$)(NO$_2$)](PF$_6$)$_2$ (**5**)	77 K, glassy solution	472, 497sh, 506, 543, 586, 632

diimine vibrational modes. The emission bandshapes are very similar, confirming their relative insensitivity to the donor properties of the monodentate ligands. In contrast, the deprotonated complexes do not exhibit emission in the visible region in a room-temperature solution, which is in keeping with observations for other platinum(II) polypyridyl complexes with dangling nucleophiles.[26,27,29,80,85] This result is consistent with stabilization of weakly emissive CT states upon deprotonation, as well as the notion that interactions of the d^8-electron metal center with nucleophiles can quench luminescence.

Electrochemistry. To assess the influence of the dangling piperidyl and piperidinium groups on the redox properties of Pt(phen)(pip$_2$NCNH$_2$)Cl^{2+}, Pt(phen)(pip$_2$NCNH$_2$)Br^{2+}, and Pt(phen)(pip$_2$NCNH$_2$)I^{2+}, cyclic voltammograms (CVs) were recorded of samples dissolved in CH_2Cl_2 with 0.1 M TBAPF$_6$. The CV of Pt(phen)(pip$_2$NCNH$_2$)Cl^{2+} (0.025 V/s, gold working electrode) shows no evidence of oxidation at potentials <1.5 V vs Ag/AgCl, and this is consistent with stabilization of the amine groups by protonation. Similarly, no reduction processes are observed at potentials >−0.5 V. We were surprised to find that deprotonation of the piperidinium groups did not effectively turn on the reversible two-electron chemistry observed for Pt(tpy)(pip$_2$NCN)$^+$. The addition of 0.5 equiv of TBAOH resulted in the appearance of an irreversible wave characterized by an anodic peak (E_{pc}), maximizing near 0.8 V (Figure 6). The addition of 1 equiv of base caused a significant increase in the current near 0.8 V, as well as the appearance of an oxidation process at 0.5 V and an apparent back-reduction process near 0.16 V. Further addition of base (up to 2 equiv in total) caused a significant increase in the current associated with the ∼0.5 V feature *at the expense* of the current associated with the ∼0.8 V process. The peak-to-peak separation (ΔE_p) between the anodic (E_{pa}, 0.5 V) and cathodic (E_{pc}, 0.2 V) peaks was >200 mV at all scan rates, indicating poor electrochemical reversibility. The ratio of the cathodic to anodic peak currents (i_{pa}/i_{pc}) was 2.75 at 0.01 V/s, suggesting that the electrochemical product is chemically unstable. Faster scan rates improved the chemical reversibility, but even at scan rates up to 1.0 V/s, there was significant decomposition (i_{pa}/i_{pc}, 1.25). Thus, under all conditions, it was apparent that this process is less chemically and electrochemically reversible than that observed for Pt(tpy)(pip$_2$NCN)$^+$ (e.g., ΔE_p, 43 mV; i_{pa}/i_{pc}, 1.00 at 0.01 V/s).[26,27] The CVs of both Pt(phen)(pip$_2$NCN)Br and Pt(phen)(pip$_2$NCN)I exhibit similar oxidation processes near 0.5 V. However, in the cathodic sweep, the behavior of these adducts is more complicated, giving rise to multiple waves (Figures S12−S14 in the Supporting Information). The exact nature of the 0.8 V process is not certain. A similar wave appears in the CV of Pt(phen)(pipNC)(pipNHC)$^+$ (E_{pa}, 0.8 V;

dx.doi.org/10.1021/ic202462a | *Inorg. Chem.* 2012, 51, 4572−4587

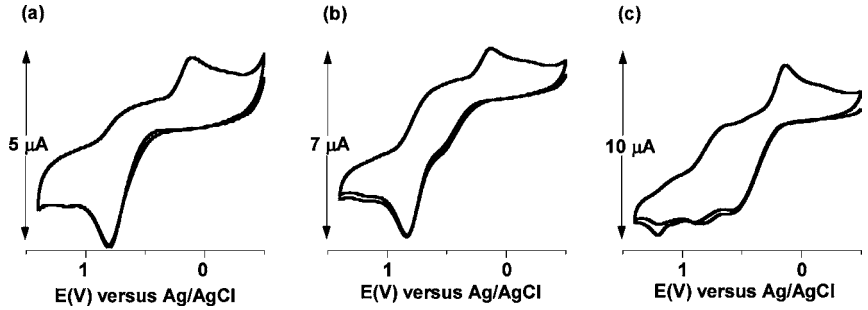

Figure 6. CVs of 1.0 μM **1** in 0.1 M $TBAPF_6/CH_2Cl_2$ at 0.1 V/s: (a) 0.5 equiv of TBAOH; (b) 1.0 equiv of TBAOH; (c) 2.0 equiv of TBAOH.

0.01 V/s),[29] and both pip_2NCNBr and $pip_2NCNBrH_2^{2+}$ exhibit an adsorption wave near 0.8 V. In contrast, $Pt(pip_2NCN)X$ (X = Cl, Br, or I), for which the piperidyl groups are protected by coordination with the metal center, is irreversibly oxidized near 1.15, 1.05, and 0.90 V vs Ag/AgCl, respectively; similar results have been reported for $Pt(Me_4NCN)Cl$ (0.76 V vs Fc/Fc^+, 0.1 M $TBAPF_6/THF$).[86,87]

The anodic wave near 0.5 V clearly arises from $Pt(phen)(pip_2NCN)(L)$. A similar wave was observed for $Pt(phen)(pipNC)_2$ (E_{pa}, 0.45 V) under identical conditions.[29] By analogy to $Pt(tpy)(pip_2NCN)^+$, we tentatively assign this to a metal-centered process that involves the dangling piperidyl groups. For $Pt(phen)(pip_2NCN)Cl$, the values of the anodic (E_{pa}, ~0.5 V) and cathodic (E_{pc}, 0.2 V) peak potentials show a characteristic dependence on the sweep rate, with E_{pa} undergoing a substantial anodic shift with increasing scan rate compared to the cathodic shift of E_{pc}. E_{pa} increases from 0.46 to 0.60 V as the scan rate is varied from 0.025 to 1.0 V/s; over the same scan rate range, E_{pc} decreases by only 0.05 mV. This pattern of behavior is very similar to that found for cooperative two-electron reagents[26,27,88−90] and is consistent with the formation of an organized structure, such as a five- or six-coordinate complex with intramolecular Pt−piperidyl interactions, prior to or during anodic electron transfer. Such interactions are likely to be weaker in the case of $Pt(phen)(pip_2NCN)Cl$ because of the lower electrophilicity of the metal center compared to $Pt(tpy)(pip_2NCN)^+$. Thus, the comparatively lower platinum acidity of $Pt(phen)(pip_2NCN)L$ appears to account for its reduced electrochemical reversibility.

The involvement of the piperidyl groups is reflected in the cathodic shift relative to the $Pt^{III/II}$ couple of $Pt(phen)(mesityl)_2$ (0.45 V vs Fc/Fc^+; 0.1 M $TBAPF_6/THF$),[79] in which there are no amine groups available to interact at the open coordination sites. Given the strong donor properties of the mesityl groups and the well-characterized relative influence of the phenyl and chloro donor groups on $Ru^{III/II}$ couples,[91] we conclude that $Pt(phen)(mesityl)_2$ provides a conservative lower limit (i.e., ≥1.0 V vs Ag/AgCl) on the $Pt^{III/II}$ couple for $Pt(phen)(pip_2NCN)Cl$ in the absence of apical nucleophile interactions. Thus, the dangling amine groups stabilize the oxidized complex by at least 0.5 V. For $Pt(phen)(pip_2NCN)Cl$, if the anodic (0.5 V vs Ag/AgCl) and cathodic (0.2 V Ag/AgCl) peak potentials are taken as the upper and lower limits of the formal redox potential ($E_{1/2}$), then it would appear that $E_{1/2}$ is surprisingly similar to the $Pt^{IV/II}$ redox couple of $Pt(tpy)(pip_2NCN)^+$ (0.4 V vs Ag/AgCl; 0.1 M $TBAPF_6/CH_3CN$).[26,27] For example, from the relative influence of chloride compared to a pyridyl ligand on the $Ru^{III/II}$ couple of six-coordinate complexes,[92−95] we would anticipate a 0.4−0.5 V cathodic shift in the Pt-centered couple upon substitution of a chloride group for a pyridyl group (i.e., $Pt(phen)(pip_2NCN)Cl$ vs $Pt(tpy)(pip_2NCN)^+$; Scheme 1). At least in part, the apparent disagreement can be attributed to the non-Nernstian electrochemistry of $Pt(phen)(pip_2NCN)Cl$, which cannot be expected to provide a reliable estimate of $E_{1/2}$. Nevertheless, this is clearly not the entire explanation, and the influence of ligand substituents on the relative stabilities of the platinum $d^6/d^7/d^8$-electron configurations remains an area of ongoing investigation.

CONCLUSIONS

The accumulated data indicate that the halide/pseudohalide group (L^-) and the metal center in $Pt(phen)(pip_2NCNH_2)(L)^{2+}$ are capable of behaving as Brønsted bases, forming intramolecular NH···Pt/L interactions involving the piperidinium groups. In the case of the protonated adducts, the geometries of the NH···Pt interactions are consistent with hydrogen bonding to the metal, rather than three-center/two-electron agostic interactions.[26,68,96] The involvement of the halide/pseudohalide group is reflected in the tendency of the NH group to be directed toward the Pt−L bond, such that the proton has the appearance of bridging the two bonded proton acceptors. In conjunction with our earlier report,[29] the CT spectra of this series of complexes demonstrate that electronic spectroscopy is a powerful and exceptionally sensitive method for probing intramolecular NH···Pt and NH···L interactions. Specifically, the NH···Pt/L interactions have a significant and unambiguous impact on the electronic spectra of these complexes, strongly destabilizing MLCT states and inducing an anodic shift in metal-centered redox processes. By contrast, deprotonation results in a new low-energy absorption band and significant stabilization of higher oxidation states. These latter properties are qualitatively similar to our observations for a series of related systems with dangling nucleophiles.[26,27,29,80] Interestingly, the chemical and electrochemical reversibility of the $Pt(phen)(pip_2NCN)(L)$ adducts is substantially lower than that of $Pt(tpy)(pip_2NCN)^+$. It is apparent that the mere availability of dangling piperidyl groups that can stabilize a six-coordinate d^6-electron product, such as in $Pt(phen)(pip_2NCN)(L)$ and $Pt(diimine)(pipNC)_2$, is not sufficient to meet the requirements for reversible two-electron transfer. We believe that a contributing factor is the lower electrophilicity of the metal center in the $Pt(phen)(pip_2NCN)(L)$ series, which is anticipated to decrease the tendency of the dangling piperidyl groups to interact at the open coordination sites compared to $Pt(tpy)(pip_2NCN)^+$. These interactions are expected to preorganize the complex for electron transfer, thereby increasing the rate of heterogeneous electron transfer and conversion to the d^6-electron product. In addition, it would appear that the combination of a monodentate halide ligand

dx.doi.org/10.1021/ic202462a | Inorg. Chem. 2012, 51, 4572−4587

and a diimine ligand favors chemical steps following electron transfer (leading to decomposition of the complex) that are comparatively slow in the case of a more conformationally restricted meridional-coordinating tpy ligand.

■ ASSOCIATED CONTENT

Supporting Information

Figures S1−S14 and crystallographic data in CIF format for all compounds. This material is available free of charge via the Internet at http://pubs.acs.org.

■ AUTHOR INFORMATION

Corresponding Author

*E-mail: bill.connick@uc.edu. Fax: (+1) 513-556-9239.

Notes

The authors declare no competing financial interest.

■ ACKNOWLEDGMENTS

Funding for the SMART6000 CCD diffractometer was through NSF-MRI Grant CHE-0215950. W.B.C. thanks the National Science Foundation (Grant CHE-0134975) for their generous support and the Arnold and Mabel Beckman Foundation for a Young Investigator Award. S.C. thanks the University of Cincinnati University Research Council for a summer fellowship and the University of Cincinnati Industrial Affiliates Program for their generous support. We also thank Dr. Allen G. Oliver, Dr. Hershel Jude, and the late Professor Richard C. Elder for helpful discussions and Drs. Larry Sallans and Stephen Macha for assistance with MS measurements. Synchrotron data were collected through the SCrALS (Service Crystallography at Advanced Light Source) project at Beamline 11.3.1 at the Advanced Light Source (ALS), Lawrence Berkeley National Laboratory. The ALS is supported by the U.S. Department of Energy, Office of Energy Sciences, under Contract DE-AC02-05CH11231.

■ REFERENCES

(1) Young, J. F.; Osborn, J. A.; Jardine, F. H.; Wilkinson, G. *Chem. Commun.* **1965**, 131−132.

(2) Shilov, A. E.; Shul'pin, G. B. *Russ. Chem. Rev.* **1987**, *56*, 442−464.

(3) Boucher, H. A.; Lawrance, G. A.; Lay, P. A.; Sargeson, A. M.; Bond, A. M.; Sangster, D. F.; Sullivan, J. C. *J. Am. Chem. Soc.* **1983**, *105*, 4652−4661.

(4) Finke, R. G.; Voegeli, R. H.; Laganis, E. D.; Boekelheide, V. *Organometallics* **1983**, *2*, 347−350.

(5) Bowyer, W. J.; Geiger, W. E.; Boekelheide, V. *Organometallics* **1984**, *3*, 1079−1086.

(6) Voegeli, R. H.; Kang, H. C.; Finke, R. G.; Boekelheide, V. *J. Am. Chem. Soc.* **1986**, *108*, 7010−7016.

(7) Rawle, S. C.; Yagbasan, R.; Prout, K.; Cooper, S. R. *J. Am. Chem. Soc.* **1987**, *109*, 6181−6182.

(8) Blake, A. J.; Gould, R. O.; Holder, A. J.; Hyde, T. I.; Lavery, A. J.; Odulate, M. O.; Scrhöder, M. *J. Chem. Soc., Dalton Trans.* **1987**, 118−120.

(9) Blake, A. J.; Gordon, L. M.; Holder, A. J.; Hyde, T. I.; Reid, G.; Schroder, M. *J. Chem. Soc., Chem. Commun.* **1988**, 1452−1454.

(10) McAuley, A.; Whitcombe, T. W. *Inorg. Chem.* **1988**, *27*, 3090−3099.

(11) Bowyer, W. J.; Geiger, W. E. *J. Electroanal. Chem.* **1988**, *239*, 253−271.

(12) Merkert, J.; Nielson, R. M.; Weaver, M. J.; Geiger, W. E. *J. Am. Chem. Soc.* **1989**, *111*, 7084−7087.

(13) Edwin, J.; Geiger, W. E. *J. Am. Chem. Soc.* **1990**, *112*, 7104−7112.

(14) Plitzko, K. D.; Rapko, B.; Gollas, B.; Wehrle, G.; Weakley, T.; Pierce, D. T.; Geiger, W. E. Jr.; Haddon, R. C.; Boekelheide, V. *J. Am. Chem. Soc.* **1990**, *112*, 6545−6556.

(15) Cooper, S. R.; Rawle, S. C.; Yagbasan, R.; Watkin, D. J. *J. Am. Chem. Soc.* **1991**, *113*, 1600−1604.

(16) Blake, A. J.; Crofts, R. D.; Scrhöder, M. *J. Chem. Soc., Dalton Trans.* **1993**, 2259−2260.

(17) Grant, G. J.; Spangler, N. J.; Setzer, W. N.; VanDerveer, D. G.; Mehne, L. F. *Inorg. Chim. Acta* **1996**, *246*, 31−40.

(18) Blake, A. J.; Roberts, Y. V.; Schröder, M. *J. Chem. Soc., Dalton Trans.* **1996**, *9*, 1885−1895.

(19) Brown, K. N.; Hockless, D. C. R.; Sargeson, A. M. *J. Chem. Soc., Dalton Trans.* **1999**, 2171−2176.

(20) Matsumoto, M.; Funahashi, S.; Takagi, H. D. *Z. Naturforsch., B: Chem. Sci.* **1999**, *54*, 1138−1146.

(21) Connelly, N. G.; Emslie, D. J. H.; Geiger, W. E.; Hayward, O. D.; Linehan, E. B.; Orpen, A. G.; Quayle, M. J.; Rieger, P. H. *J. Chem. Soc., Dalton Trans.* **2001**, 670−683.

(22) Grant, G. J.; Carter, S. M.; LeBron, R. A.; Poullaos, I. M.; VanDerveer, D. G. *J. Organomet. Chem.* **2001**, *637−639*, 683−690.

(23) Brown, K. N.; Geue, R. J.; Hambley, T. W.; Hockless, D. C. R.; Rae, A. D.; Sargeson, A. M. *Org. Biomol. Chem.* **2003**, *1*, 1598−1608.

(24) Geiger, W. E.; Ohrenberg, N. C.; Yeomans, B.; Connelly, N. G.; Emslie, D. J. H. *J. Am. Chem. Soc.* **2003**, *125*, 8680−8688.

(25) Grant, G. J.; Patel, K. N.; Helm, M. L.; Mehne, L. F.; Klinger, D. W.; VanDerveer, D. G. *Polyhedron* **2004**, *23*, 1361−1369.

(26) Jude, H.; Krause Bauer, J. A.; Connick, W. B. *J. Am. Chem. Soc.* **2003**, *125*, 3446−3447.

(27) Jude, H.; Carroll, G. T.; Connick, W. B. *Chemtracts* **2003**, *16*, 13−22.

(28) Marcus, R. A. *Annu. Rev. Phys. Chem.* **1964**, *15*, 155.

(29) Chatterjee, S.; Krause, J. A.; Oliver, A. G.; Connick, W. B. *Inorg. Chem.* **2010**, *49*, 9798−9808.

(30) McDermott, J. X.; White, J. F.; Whitesides, G. M. *J. Am. Chem. Soc.* **1976**, *98*, 6521−6528.

(31) Price, J. H.; Williamson, A. N.; Shramm, R. F.; Wayland, B. B. *Inorg. Chem.* **1972**, *11*, 1280−1284.

(32) Kiyooka, S.; Tada, M.; Kan, S.; Fujio, M. *Bull. Chem. Soc. Jpn.* **1996**, *69*, 2595−2601.

(33) Schimmelpfennig, U.; Zimmering, R.; Schleinitz, K. D.; Stoesser, R.; Wenschuh, E.; Baumeister, U.; Hartung, H. *Z. Anorg. Allg. Chem.* **1993**, *619*, 1931−1938.

(34) Chan, K. S.; Tse, A. K.-S. *Synth. Commun.* **1993**, *23*, 1929−1934.

(35) Jude, H.; Krause Bauer, J. A.; Connick, W. B. *Inorg. Chem.* **2002**, *41*, 2275−2281.

(36) Jude, H. Ph.D. Dissertation. University of Cincinnati, Cincinnati, OH, 2004.

(37) Kissinger, P. T.; Heineman, W. R. *J. Chem. Educ.* **1983**, *60*, 702−706.

(38) Rotondo, E.; Bruschetta, G.; Bruno, G.; Rotondo, A.; Di Pietro, M. L.; Cusumano, M. *Eur. J. Inorg. Chem.* **2003**, 2612−2618.

(39) Clement, O.; Macartney, D. H.; Buncel, E. *Inorg. Chim. Acta* **1997**, *264*, 117−124.

(40) Margiotta, N.; Fanizzi, F. P.; Kobe, J.; Natile, G. *Eur. J. Inorg. Chem.* **2001**, 1303−1310.

(41) Margiotta, N.; Papadia, P.; Fanizzi, F. P.; Natile, G. *Eur. J. Inorg. Chem.* **2003**, 1136−1144.

(42) Linert, W.; Jameson, R. F.; Taha, A. *J. Chem. Soc., Dalton Trans.* **1993**, 3181−3186.

(43) Brammer, L.; Charnock, J. M.; Goggin, P. L.; Goodfellow, R. J.; Orpen, A. G.; Koetzle, T. F. *J. Chem. Soc., Dalton Trans.* **1991**, 1789−1798.

(44) Canty, A. J.; van Koten, G. *Acc. Chem. Res.* **1995**, *28*, 406−413.

(45) Casas, J. M.; Fornies, J.; Martin, A. *J. Chem. Soc., Dalton Trans.* **1997**, *9*, 1559−1563.

(46) Wehman-Ooyevaar, I. C. M.; Grove, D. M.; van der Sluis, P.; Spek, A. L.; van Koten, G. *J. Chem. Soc., Chem. Commun.* **1990**, 1367−1369.

(47) Wehman-Ooyevaar, I. C. M.; Grove, D. M.; Kooijman, H.; van der Sluis, P.; Spek, A. L.; van Koten, G. *J. Am. Chem. Soc.* **1992**, *114*, 9916−9924.
(48) Pregosin, P. S.; Rüegger, H.; Wombacher, F.; van Koten, G.; Grove, D. M.; Wehman-Ooyevaar, I. C. M. *Magn. Reson. Chem.* **1992**, *30*, 548−551.
(49) Wehman-Ooyevaar, I. C. M.; Grove, D. M.; de Vaal, P.; Dedieu, A.; van Koten, G. *Inorg. Chem.* **1992**, *31*, 5484−5493.
(50) Lacabra, M. A. C.; Canty, A. J.; Lutz, M.; Patel, J.; Spek, A. L.; Sun, H.; van Koten, G. *Inorg. Chim. Acta* **2002**, *327*, 15−19.
(51) Debaerdemaeker, T.; Hohenadel, R.; Brune, H.-A. *J. Organomet. Chem.* **1988**, *350*, 109−114.
(52) Casas, J. M.; Diosdado, B. E.; Favello, L. R.; Fornies, J.; Martin, A.; Rueda, A. J. *Dalton Trans.* **2004**, 2733−2740.
(53) Ong, C. M.; Jennings, M. C.; Puddephatt, R. J. *Can. J. Chem.* **2003**, *81*, 1196−1205.
(54) Plutino, M. R.; Scolaro, L. M.; Albinati, A.; Romeo, R. *J. Am. Chem. Soc.* **2004**, *126*, 6470−6484.
(55) Sun, Y.; Ross, N.; Zhao, S.-B.; Huszarik, K.; Jia, W.-L.; Wang, R.-Y.; Macartney, D.; Wang, S. *J. Am. Chem. Soc.* **2007**, *129*, 7510−7511.
(56) Connick, W. B.; Marsh, R. E.; Schaefer, W. P.; Gray, H. B. *Inorg. Chem.* **1997**, *36*, 913−922.
(57) Tessier, C.; Rochon, F. D. *Inorg. Chim. Acta* **2001**, *322*, 37−46.
(58) Kishi, S.; Kato, M. *Inorg. Chem.* **2003**, *42*, 8728−8734.
(59) Grzesiak, A. L.; Matzger, A. J. *Inorg. Chem.* **2007**, *46*, 453−457.
(60) Fanizzi, F. P.; Intini, F. P.; Maresca, L.; Natile, G.; Lanfranchi, M.; Tiripicchio, A. *J. Chem. Soc., Dalton Trans.* **1991**, 1007−1015.
(61) Clark, R. J. H.; Fanizzi, F. P.; Natile, G.; Pacifico, C.; van Rooyen, C. G.; Tocher, D. A. *Inorg. Chim. Acta* **1995**, *235*, 205−213.
(62) Capitelli, F.; Margiotta, N.; Moliterni, A. G. G.; Natile, G. *Z. Kristallogr.* **2002**, *217*, 492−496.
(63) Jude, H.; Krause Bauer, J. A.; Connick, W. B. *Inorg. Chem.* **2004**, *43*, 725−733.
(64) Jude, H.; Krause Bauer, J. A.; Connick, W. B. *Inorg. Chem.* **2005**, *44*, 1211−1220.
(65) Bondi, A. *J. Phys. Chem.* **1964**, *68*, 441−451.
(66) Hambley, T. W. *Inorg. Chem.* **1998**, *37*, 3767−3774.
(67) Albinati, A.; Lianza, F.; Pregosin, P. S.; Mueller, B. *Inorg. Chem.* **1994**, *33*, 2522−2526.
(68) Yao, W.; Eisenstein, O.; Crabtree, R. H. *Inorg. Chim. Acta* **1997**, *254*, 105−111.
(69) Davies, M. S.; Fenton, R. R.; Huq, F.; Ling, E. C. H.; Hambley, T. W. *Aust. J. Chem.* **2000**, *53*, 451−456.
(70) Albrecht, M.; Dani, P.; Lutz, M.; Spek, A. L.; van Koten, G. *J. Am. Chem. Soc.* **2000**, *122*, 11822−11833.
(71) Jin, V. X.; Ranford, J. D. *Inorg. Chim. Acta* **2000**, *304*, 38−44.
(72) Miskowski, V. M.; Houlding, V. H. *Inorg. Chem.* **1989**, *28*, 1529−1533.
(73) Connick, W. B.; Miskowski, V. M.; Houlding, V. H.; Gray, H. B. *Inorg. Chem.* **2000**, *39*, 2585−2592.
(74) Fleeman, W. D.; Connick, W. B. *Comments Inorg. Chem* **2002**, *23*, 205−230.
(75) Chan, C.; Cheng, L.-K.; Che, C.-M. *Coord. Chem. Rev.* **1992**, *132*, 87−97.
(76) Tanaka, M.; Nagai, T.; Miki, E. *Inorg. Chem.* **1989**, *28*, 1704−1706.
(77) Sondaz, E.; Gourdon, A.; Launay, J.-P.; Bonvoisin, J. *Inorg. Chim. Acta* **2001**, *316*, 79−88.
(78) Pipes, D. W.; Meyer, T. J. *Inorg. Chem.* **1984**, *23*, 2466−2472.
(79) Klein, A.; McInnes, E. J. L.; Kaim, W. *J. Chem. Soc., Dalton Trans.* **2002**, 2371−2378.
(80) Green, T. W.; Lieberman, R.; Mitchell, N.; Krause, J. A.; Connick, W. B. *Inorg. Chem.* **2005**, *44*, 1955−1965.
(81) DePriest, J.; Zheng, G. Y.; Goswami, N.; Eichhorn, D. M.; Woods, C.; Rillema, D. P. *Inorg. Chem.* **2000**, *39*, 1955−1963.
(82) DeArmond, M. K.; Carlin, C. M.; Huang, W. L. *Inorg. Chem.* **1980**, *19*, 62−67.
(83) Ohno, T.; Kato, S. *Bull. Chem. Soc. Jpn.* **1974**, *47*, 2953−2957.
(84) Flynn, C. M.; Demas, J. N. *J. Am. Chem. Soc.* **1974**, *96*, 1959−1960.
(85) Chatterjee, S.; Krause, J. A.; Connick, W. B.; Genre, C.; Rodrigue-Witchel, A.; Reber, C. *Inorg. Chem.* **2010**, *49*, 2808−2815.
(86) Back, S.; Gossage, R. A.; Lutz, M.; del Rio, I.; Spek, A. L.; Heinrich, L.; van Koten, G. *Organometallics* **2000**, *19*, 3296−3304.
(87) Back, S.; Lutz, M.; Spek, A. L.; Lang, H.; van Koten, G. *J. Organomet. Chem.* **2001**, *620*, 227−234.
(88) Uhrhammer, D.; Schultz, F. A. *J. Am. Chem. Soc.* **2002**, *106*, 11630−11636.
(89) Uhrhammer, D.; Schultz, F. A. *Inorg. Chem.* **2002**, *43*, 7389−7395.
(90) Fernandes, J. B.; Zhang, L. Q.; Schultz, F. A. *J. Electroanal. Chem.* **1991**, *297*, 145−161.
(91) Reveco, P.; Cherry, W. R.; Medley, J.; Garber, A.; Gale, R. J.; Selbin, J. *Inorg. Chem.* **1986**, *25*, 1842−1845.
(92) Callahan, R. W.; Brown, G. M.; Meyer, T. J. *Inorg. Chem.* **1975**, *14*, 1443−1453.
(93) Constable, E. C.; Hannon, M. J. *Inorg. Chim. Acta* **1993**, *211*, 101−110.
(94) Suen, H. F.; Wilson, S. W.; Pomerantz, M.; Walsh, J. L. *Inorg. Chem.* **1989**, *28*, 786−791.
(95) Lever, A. B. P. *Inorg. Chem.* **1990**, *29*, 1271−1285.
(96) Brammer, L.; McCann, M. C.; Bullock, R. M.; McMullan, R. K.; Sherwood, P. *Organometallics* **1992**, *11*, 2339−2341.